Most recent CMB map from the Planck satellite

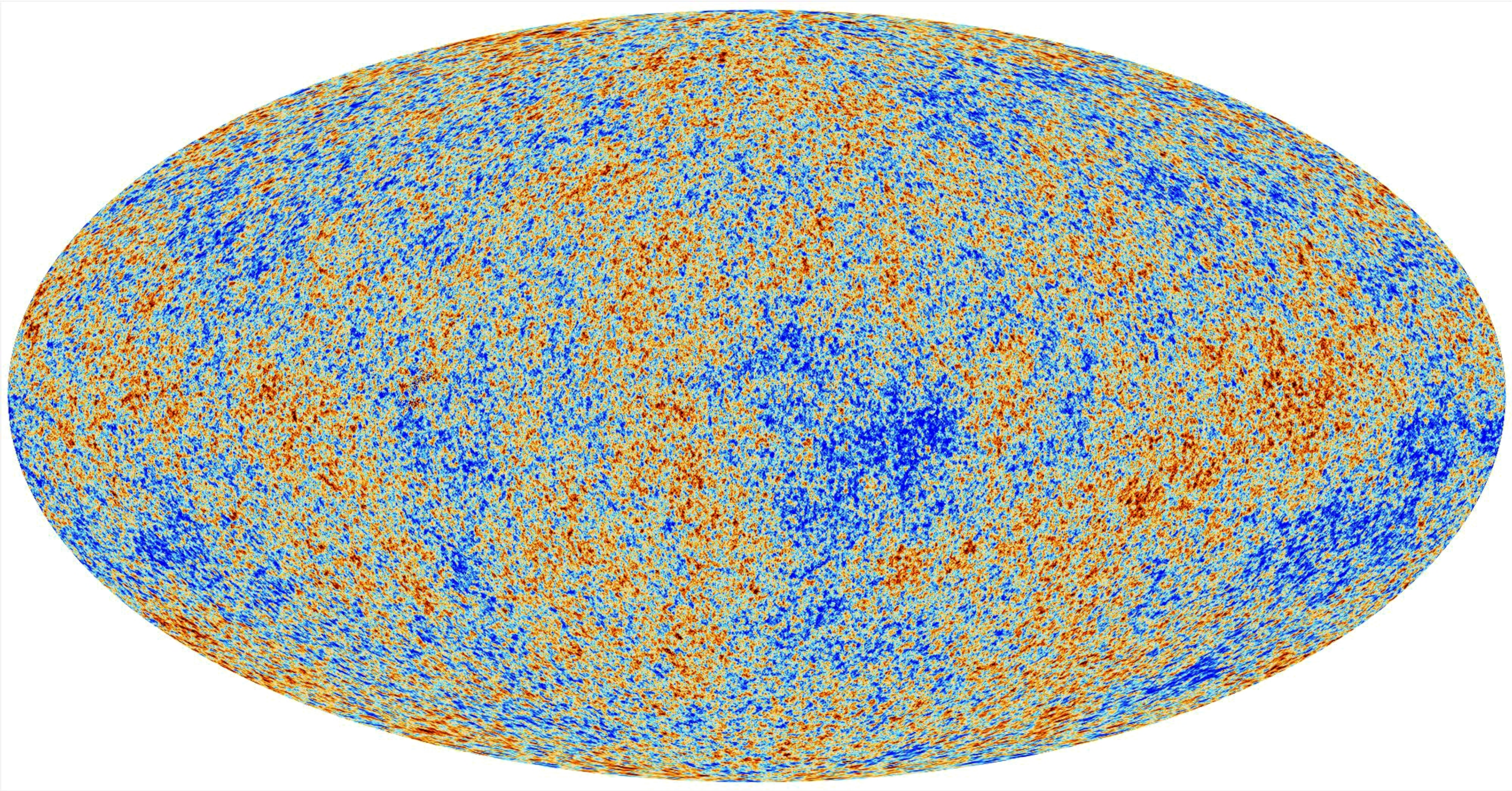

THEORY OF THE GROWTH OF PERTURBATIONS

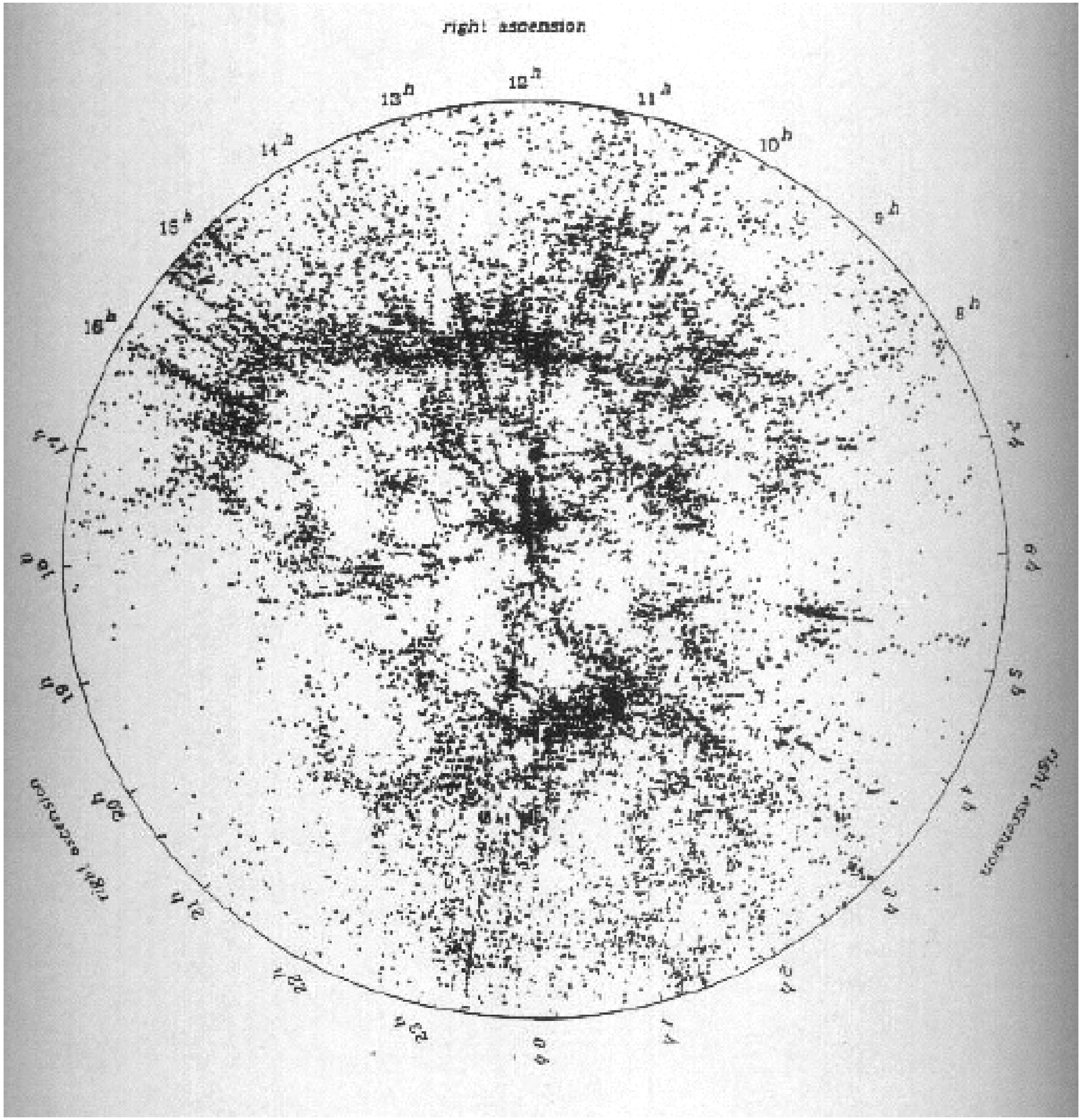

The theory of how the tiny (1/100,000) density fluctuations that we see imprinted on the CMB radiation at z=1300-1100 grow to become the galaxies we see today.

DEFINE DENSITY FLUCTUATION FIELD δ:

$$\delta = (\rho - \langle\rho\rangle) / \langle\rho\rangle$$

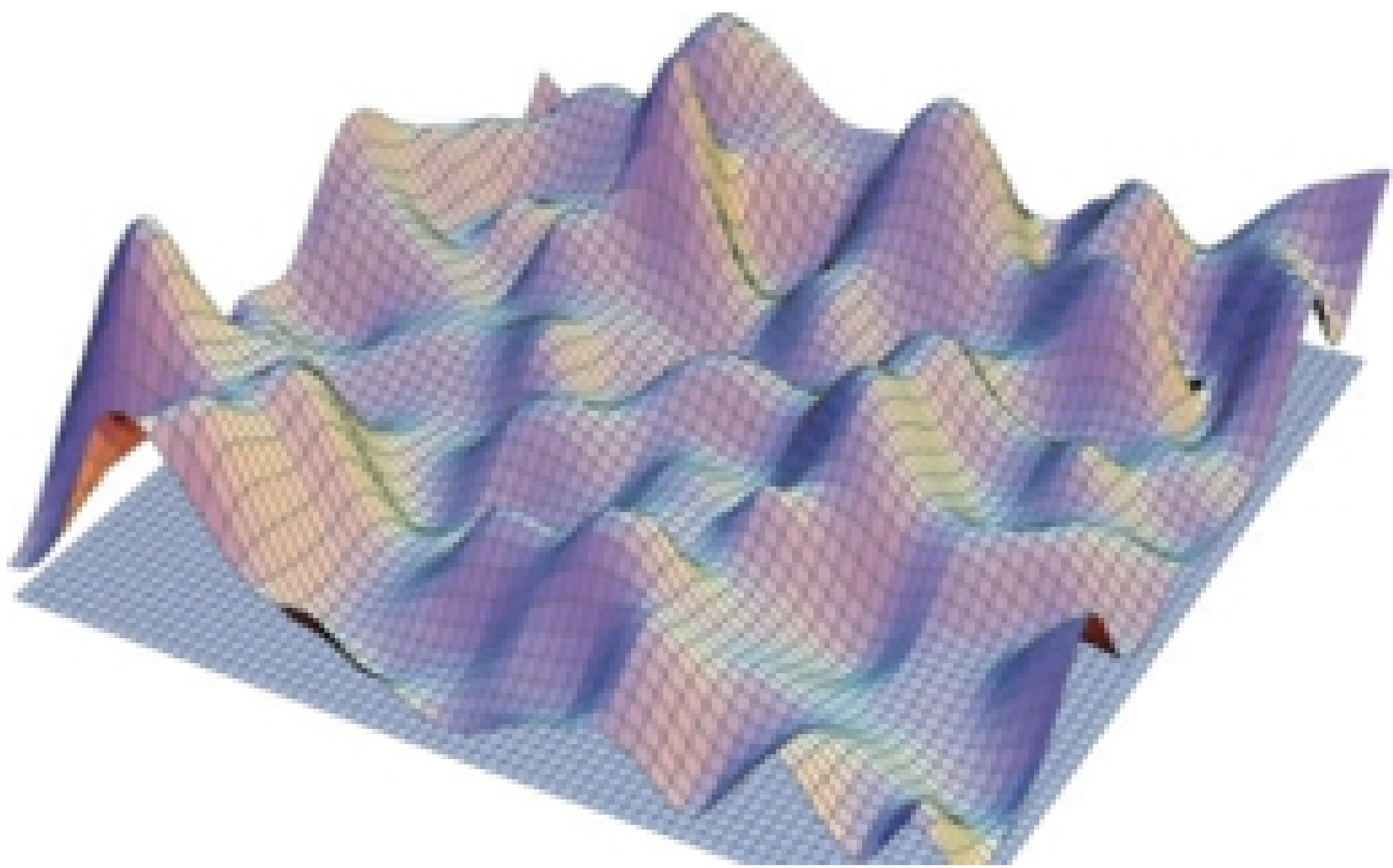

Fourier analysis of density fluctuations:

It is often convenient to consider building up a general field by the superposition of many modes. The natural tool for achieving this is via Fourier analysis. In three dimensions, the forward and inverse Fourier transforms of a field F are:

$$\delta(\mathbf{x}) = V \int \frac{d^3k}{(2\pi)^3} \, \delta(\mathbf{k}) \, e^{-i\mathbf{k}\cdot\mathbf{x}}$$

$$\delta(\mathbf{k}) = \frac{1}{V} \int d^3x \, \delta(\mathbf{x}) \, e^{i\mathbf{k}\cdot\mathbf{x}}$$

Primordial density perturbations will subsequently be modified by a variety of physical processes: growth under self-gravitation, the effect of pressure, and dissipative processes. The effect is summarized in the transfer function:

$$T_k \equiv \frac{\delta_k(z=0)}{\delta_k(z)D(z)}$$

D(z) is the growth factor between redshift z and present

The Gaussian nature of the primordial density field is preserved in its linear evolution stage, but this is not the case in the nonlinear stage. In the real density field, δ_i cannot be less than −1. This assumption does not make any practical difference as long as the fluctuations are small, but it is invalid in the nonlinear regime where the typical amplitude of the fluctuations exceeds unity.

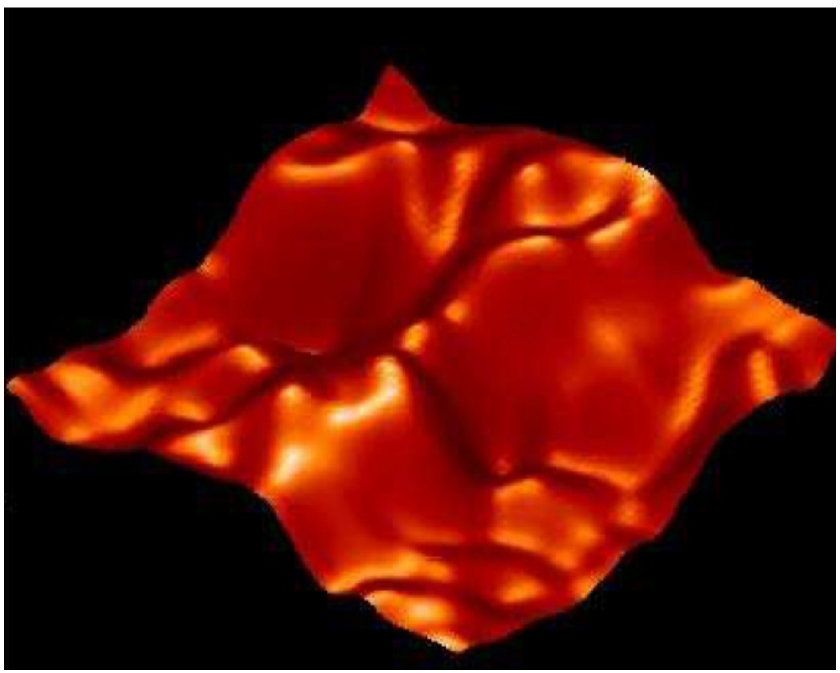

$$\delta \propto \frac{a^{-2}}{\rho} \propto \begin{cases} a^2 & \text{in the radiation dominated era} \\ a & \text{in the matter dominated era} \end{cases}$$

$$\delta = \delta_i \cdot \begin{cases} t/t_i & \text{in the radiation dominated era} \\ (t/t_i)^{2/3} & \text{in the matter dominated era} \end{cases}$$

Evolution of density perturbations into the non-linear ($\delta\rho/\rho > 1$) regime

Two approaches: APPROXIMATE METHODS and NUMERICAL SIMULATIONS

1. SPHERICAL COLLAPSE

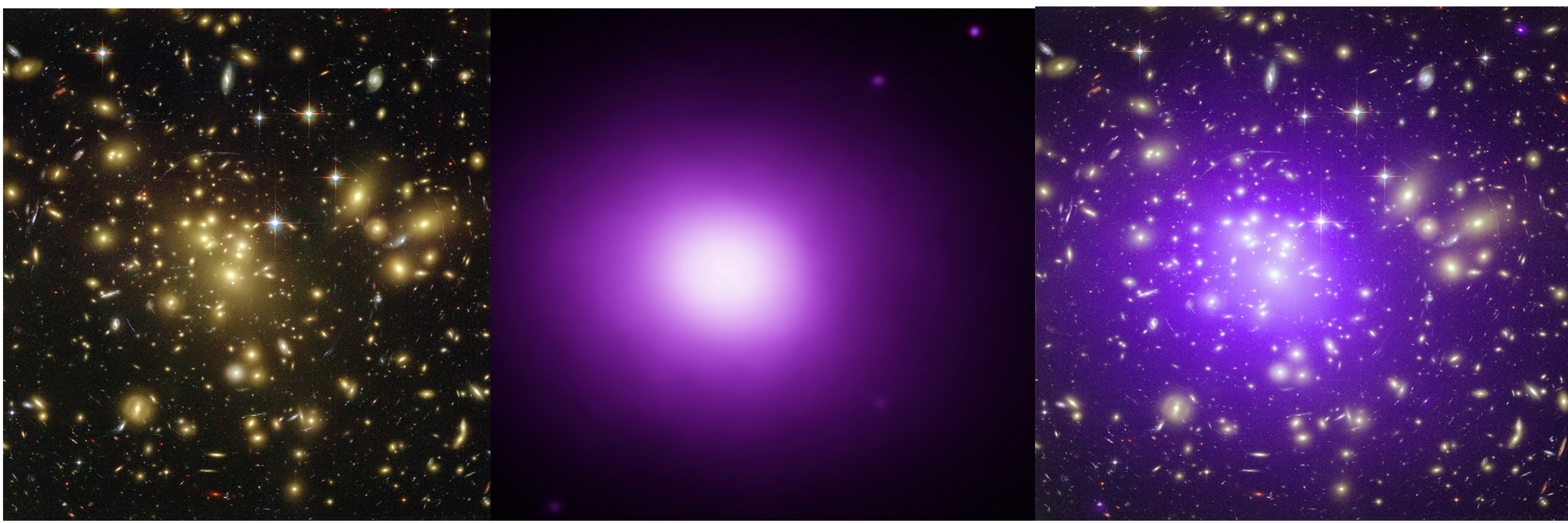

The galaxy cluster Abell 1989 seen in optical light and in X-rays

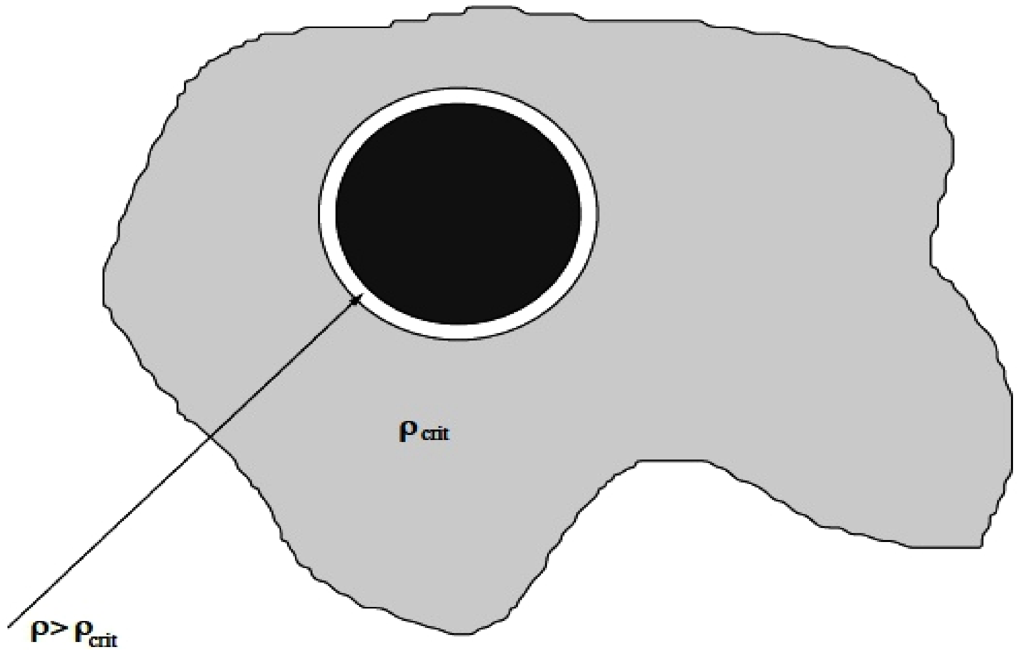

Consider the idealised case of a spherical volume where the density is infinitesimally higher than the cosmic mean.

Our density perturbation will then evolve like a closed universe with $\Omega_m = 1 + \delta$. The scale factor a(t) of such a universe reaches a maximum value a_{max} and then decreases again—in other words, our perturbation will grow to a maximum size $r=r_{max}$ at time $t=t_{max}$ and then collapse.

The Friedman equation for a closed Universe:

$$\frac{1}{a}\frac{da}{dt} = H_0\left(\Omega_{\mathrm{m},0}a^{-3} + (1-\Omega_{\mathrm{m},0})a^{-2}\right)^{1/2}$$

has a parametric solution in terms of a development angle θ:

$$\theta = H_0\,\eta\,(\Omega_{\mathrm{m},0} - 1)^{1/2}$$

so that $$r(\theta) = A(1-\cos\theta)$$

and $$t(\theta) = B(\theta - \sin\theta)$$

with $$A = r_0\frac{\Omega_{\mathrm{m},0}}{2(\Omega_{\mathrm{m},0}-1)};\quad B = \frac{1}{H_0}\frac{\Omega_{\mathrm{m},0}}{2(\Omega_{\mathrm{m},0}-1)^{3/2}}$$

the development angle θ is a scaled form of the 'conformal time' (the time travelled by a photon since the Big Bang)

The maximum size which the perturbation will grow is given by

$$\frac{dr}{d\theta} = A\sin\theta = 0$$

Which is satisfied at θ= 0, π and 2π. θ=π corresponds to the time of turn-around when the over-density reaches its maximum size before collapsing. At this time $t=t_{max}$, we have

$$r_{\rm max} = 2A = r_0 \frac{\Omega_{\rm m,0}}{\Omega_{\rm m,0} - 1}$$

and, more generally

$$\frac{r}{r_{\rm max}} = \frac{1}{2}(1 - \cos\theta)$$

$$t_{\rm max} = t(\pi) = \pi B; \quad H_0 t_{\rm max} = \frac{\pi}{2} \frac{\Omega_{\rm m,0}}{(\Omega_{\rm m,0} - 1)^{3/2}}$$

and

$$\frac{t}{t_{\rm max}} = \frac{1}{\pi}(\theta - \sin\theta)$$

The constants A and B are related through the enclosed mass

$$M = \frac{4\pi}{3} r_0^3 \Omega_{\mathrm{m},0} \rho_{\mathrm{crit}} = \frac{4\pi}{3} r_0^3 \Omega_{\mathrm{m},0} \frac{3H_0^2}{8\pi G}$$

by the simple relation $A^3 = GMB^2$

In the linear regime, we can follow the growth of the perturbation by using the McLaurin expansions for cosθ and sinθ , to yield

$$\lim_{\theta \to 0} r(\theta) = A \left(\frac{1}{2}\theta^2 - \frac{1}{24}\theta^4 \right)$$

$$\lim_{\theta \to 0} t(\theta) = B \left(\frac{1}{6}\theta^3 - \frac{1}{120}\theta^5 \right)$$

The leading order, $r = A\theta^2/2$ and $t = B\theta^3/6$, just gives the expansion of the background (i.e. outside the volume including the over-density) universe where

$$r = a = \frac{A}{2} \left(\frac{6t}{B} \right)^{2/3}$$

Our over-density grows according to the equations:

$$\frac{r}{r_{\max}} \simeq \frac{\theta^2}{4} - \frac{\theta^4}{48}, \qquad \frac{t}{t_{\max}} \simeq \frac{1}{\pi}\left(\frac{\theta^3}{6} - \frac{\theta^5}{120}\right)$$

which can be combined to give the linearized scale factor of our closed Universe:

$$\frac{a_{\mathrm{lin}}}{a_{\max}} \simeq \frac{1}{4}\left(6\pi\frac{t}{t_{\max}}\right)^{2/3}\left[1 - \frac{1}{20}\left(6\pi\frac{t}{t_{\max}}\right)^{2/3}\right]$$

Again, the first term is just the expansion of the background in a flat matter dominated universe. Including both terms in the square brackets gives the linear theory expression for the growth of a perturbation.

Our over-density grows according to the equations:

$$\frac{r}{r_{\max}} \simeq \frac{\theta^2}{4} - \frac{\theta^4}{48}, \qquad \frac{t}{t_{\max}} \simeq \frac{1}{\pi}\left(\frac{\theta^3}{6} - \frac{\theta^5}{120}\right)$$

which can be combined to give the linearized scale factor of our closed Universe:

$$\frac{a_{\rm lin}}{a_{\max}} \simeq \frac{1}{4}\left(6\pi\frac{t}{t_{\max}}\right)^{2/3}\left[1 - \frac{1}{20}\left(6\pi\frac{t}{t_{\max}}\right)^{2/3}\right]$$

Again, the first term is just the expansion of the background in a flat matter dominated universe. Including both terms in the square brackets gives the linear theory expression for the growth of a perturbation.

Throughout the evolution of the perturbation, the following relation holds:

$$1 + \delta_{\rm lin} = \left(\frac{a_{\rm back}}{a_{\rm lin}}\right)^3$$

Substituting this into the previous equation where a_{back} is given by the leading order term, and with the substitution $(1 + \delta)^{-1/3} \sim 1 - 1/3\,\delta$ valid for $\delta \ll 1$, we have:

$$\delta_{\rm lin} = \frac{3}{20}\left(6\pi\frac{t}{t_{\rm max}}\right)^{2/3}$$

At $t = t_{max}$ (turnaround) $\delta_{lin} = 1.06$

The density contrast at turnaround is:

$$1 + \delta^{\rm turn}_{\rm nonlin} = \left(\frac{a_{\rm back}}{a_{\rm max}}\right)^3 = \left[\frac{1}{4}\left(6\pi\frac{t}{t_{\rm max}}\right)^{2/3}\right]^3 = \frac{(6\pi)^2}{4^3} = 5.55$$

At $t = 2t_{max}$ (collapse) $\delta_{lin} = 1.686$

After turnaround, the evolution of the over-density mirrors the expansion phase until the object collapses at t = $2t_{max}$. At this time the linear density contrast has become

$$\delta_{\rm lin}^{\rm coll} = \delta_{\rm c} = \frac{3}{20}(12\pi)^{2/3} = 1.686$$

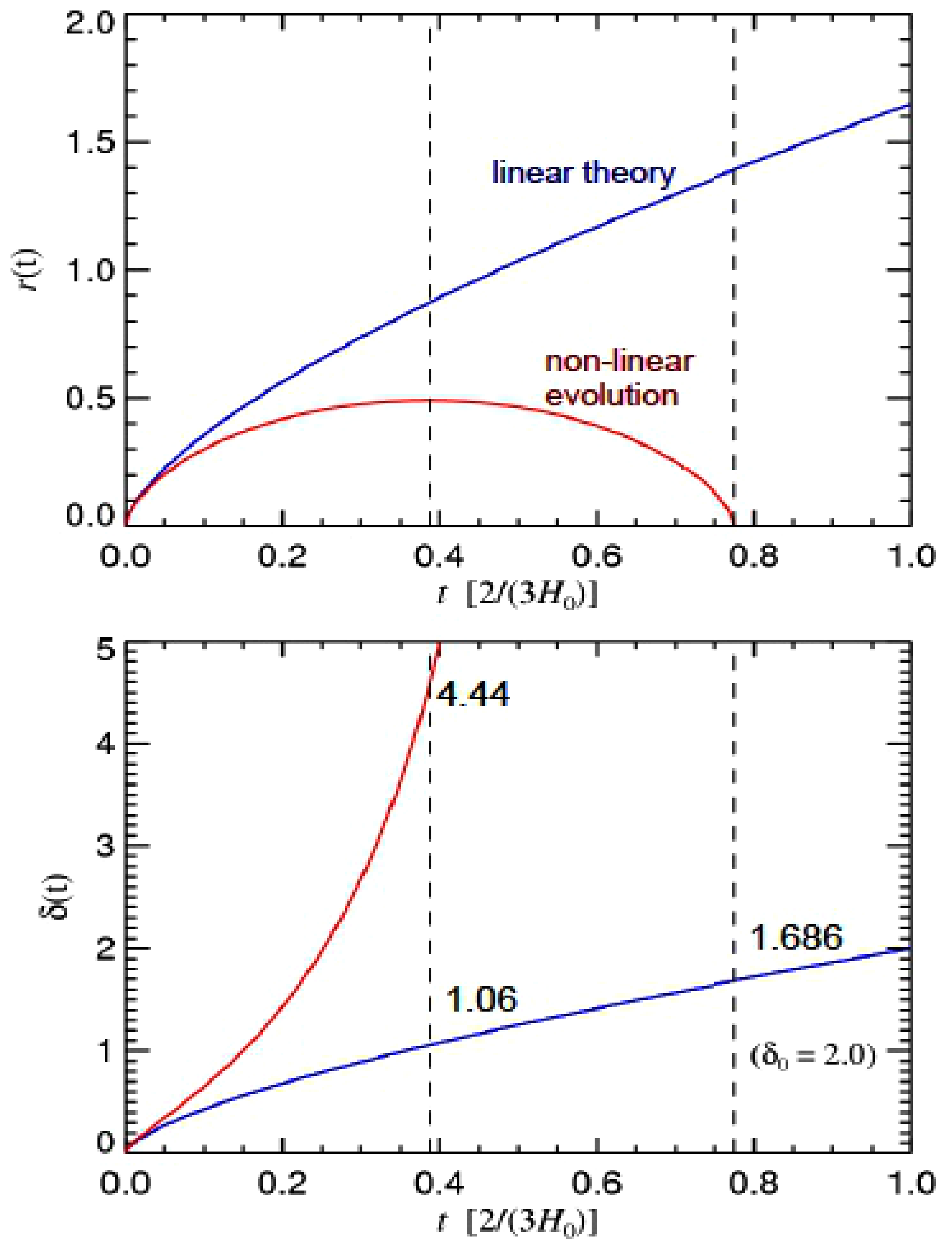

Thus, a linear density contrast δ_C ~1.7 corresponds to the epoch of complete gravitational collapse of a spherically symmetric perturbation.

This value of δc~ 1.7 is used in analytical treatments of the growth of structure in the universe, such as the Press-Schechter formalism.

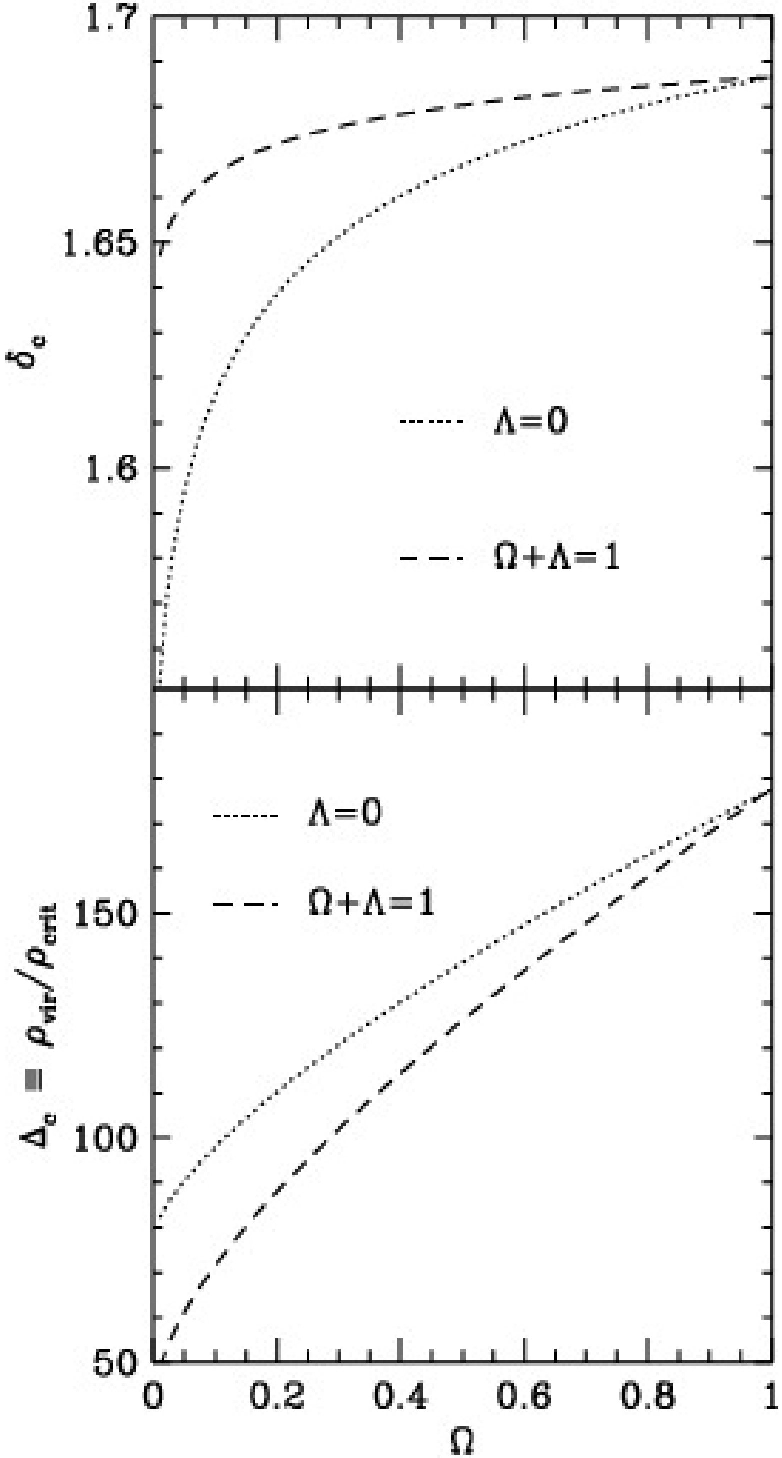

Variation in the linearly extrapolated critical density for collapse and the non-linear overdensity at virialization between flat models with and without a cosmological constant.

Virialization

A real density perturbation is neither spherical nor homogeneous. Thus, the collapse does not proceed to a point of infinite density, but reaches **virial equilibrium** at a radius $r_{vir} = 1/2\ r_{max}$.

This can be appreciated by considering the **virial theorem** (see lecture 1) $U_{vir} = -2T_{vir}$, where U and T represent the potential and kinetic energies respectively. At turnaround, the kinetic energy of the collapsing sphere is zero. From conservation of energy, we have: $U_{rmax} + T_{rmax} = U_{vir} + T_{vir}$.
Thus, $U_{rmax} = U_{vir} - 1/2U_{vir} = 1/2U_{vir}$. Since the gravitational energy of a mass M within a spherical volume of radius R is $U \sim 1/R$, it follows that $R_{turn} = 2R_{vir}$.

By this time, the density within our volume has increased by a factor of 2^3, while that of the background universe has decreased by a factor of 2^2, since $\rho \sim a^{-3}$ and $a \sim t^{2/3}$ in a matter-dominated universe. Thus, at virialization, the overdensity within our volume has grown from 5.5 to 178.

Optical(left) and X-ray(right) images of the Coma Cluster

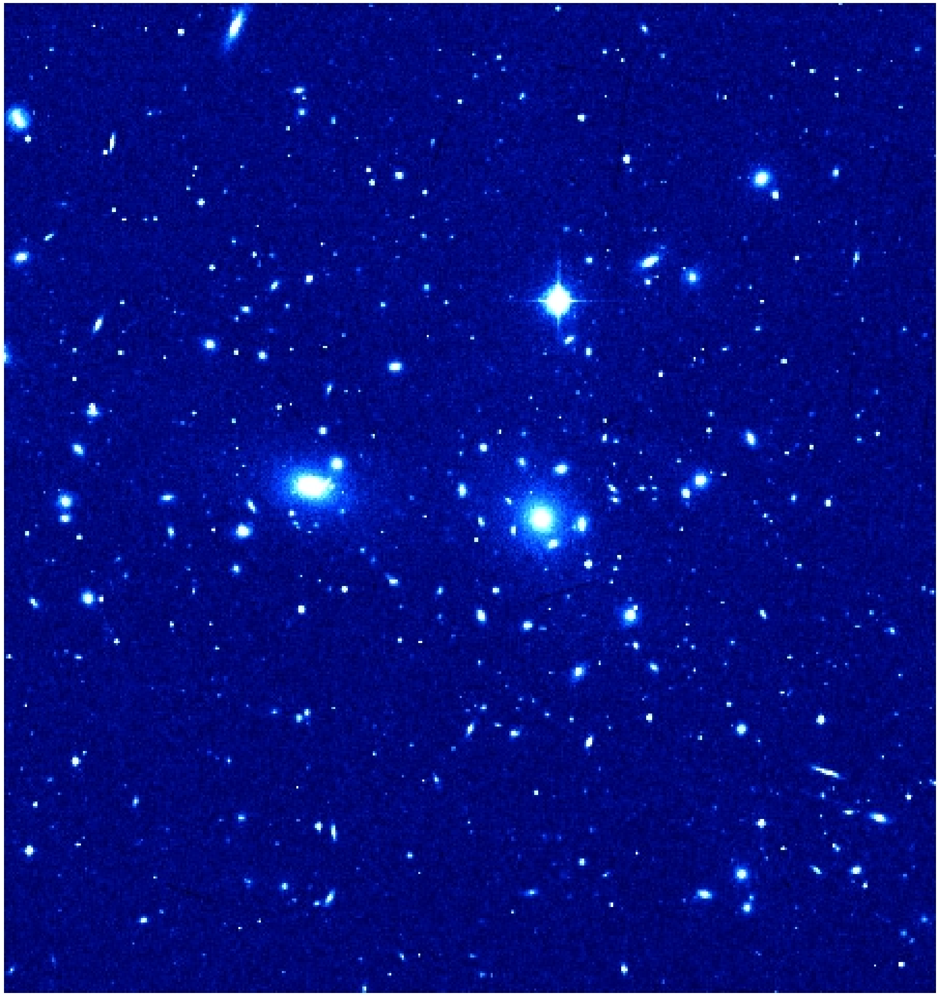

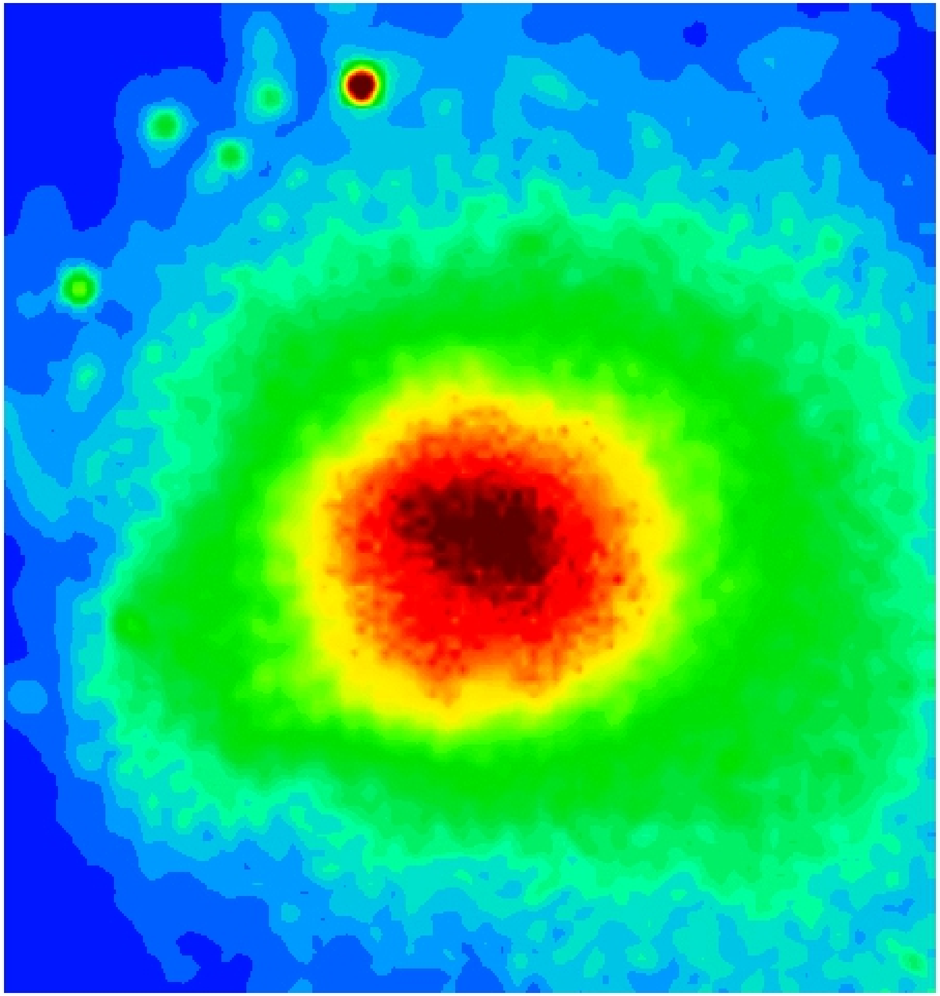

In terms of the initial co-moving radius $r_{i,com}$, we have:

$$r_{vir}^3 = \frac{1}{178} \frac{1}{(1+z_{vir})^3} r_{i,com}^3$$

The virial theorem for bound objects tells us: $v^2 = GM/r_g$

where M is the mass of the system and r_g is the radius within which the gravitational energy is $U = -GM^2/r_g$. The mass within $r_{i,com}$ is $4/3\,\pi\, r^3_{i,com}\, \rho_{m,0}$

Combining the above equations, we find that the velocity dispersion and the mass of a collapsed object are related by:

$$\left(\frac{v}{127\ \mathrm{km\ s^{-1}}}\right)^2 = \left(\frac{M}{10^{12}\, h^{-1} M_\odot}\right)^{2/3} (1+z_{vir})$$

This means that perturbations which collapse at earlier times have higher velocity dispersions for the same enclosed mass ---Higher over-densities turn around and collapse at the earlier times, when the background universe was smaller and denser, and when virialized have proportionally higher velocity dispersions.

Finally, if the matter within the volume is in hydrostatic equilibrium,we can associate a temperature to the velocity dispersion, $T \sim v^2$, and hence obtain the scaling:

$$\frac{kT}{7\ \mathrm{keV}} = \left(\frac{M}{10^{15} h^{-1} M_\odot}\right)^{2/3} (1 + z_{\mathrm{vir}})$$

Gas at such high temperatures gives rise to X-ray emission through thermal bremsstrahlung radiation (to be explained later)

Press-Schechter model for the statistics of collapsed, virialized halos in the Universe

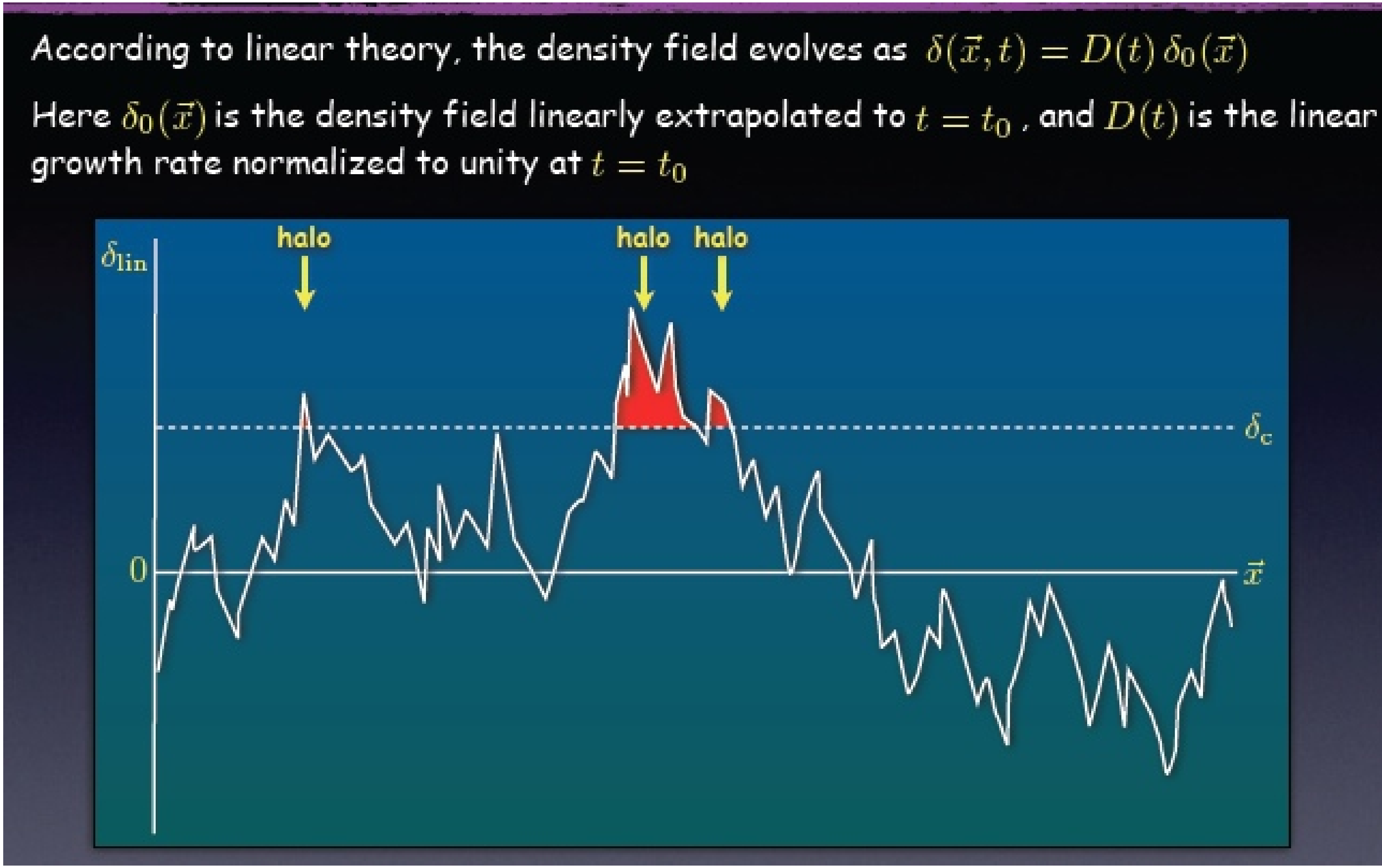

According to the spherical collapse model, regions with δ(**x**,t)>δc=1.686 will have collapsed to produce dark matter halos by time t.

If the density field is Gaussian, the probability that a given point lies in a region with $\delta > \delta_c$ is:

$$p(\delta > \delta_c \mid R) = \frac{1}{\sqrt{2\pi}\,\sigma(R)} \int_{\delta_c}^{\infty} \exp\left(-\delta^2/2\sigma^2(R)\right)\, d\delta,$$

where $\sigma(R)$ is the rms of the density field δ on scale R. The PS argument assumes that the only objects that exist at a given epoch are those that have only just reached the $\delta = \delta_c$ collapse threshold; if a point has $\delta > \delta_c$ for a given R, then it will have $\delta = \delta_c$ when filtered on some larger scale and will be counted as an object of the larger scale. The problem with this argument is that half the mass remains unaccounted for: PS therefore simply multiplying the probability by a factor 2.

The fraction of the universe condensed into objects with mass > M can then be written in the universal form

$$F(> M) = \sqrt{\frac{2}{\pi}} \int_{\nu_c}^{\infty} \exp(-\nu^2/2)\, d\nu$$

where $\nu_c = \delta_c/\sigma(M)$ is the threshold in units of the rms density fluctuation andM is the mass contained in a sphere of co-moving radius R in a homogeneous universe.

The probability of a point in space forming as mass between M and M + dM is dF/dM. We can write this result in terms of the multiplicity functior

$$\frac{M^2 f(M)}{\rho_0} = \frac{dF}{d\ln M} = \left|\frac{d\ln\sigma}{d\ln M}\right| \sqrt{\frac{2}{\pi}}\,\nu\,\exp\left(-\frac{\nu^2}{2}\right)$$

which is the fraction of the mass carried by objects in a unit range of lnM.

z = 0,1,2,3,4,5

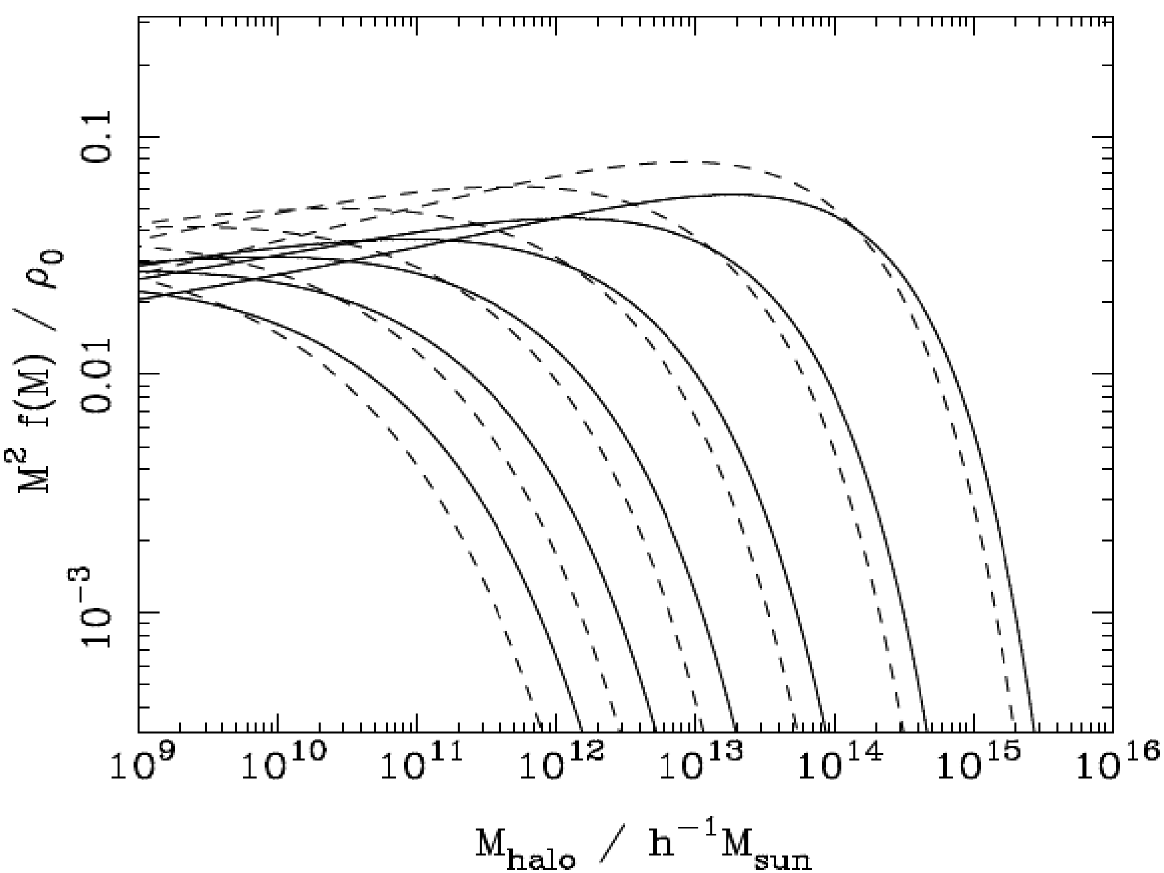

Comparison with N-body simulations

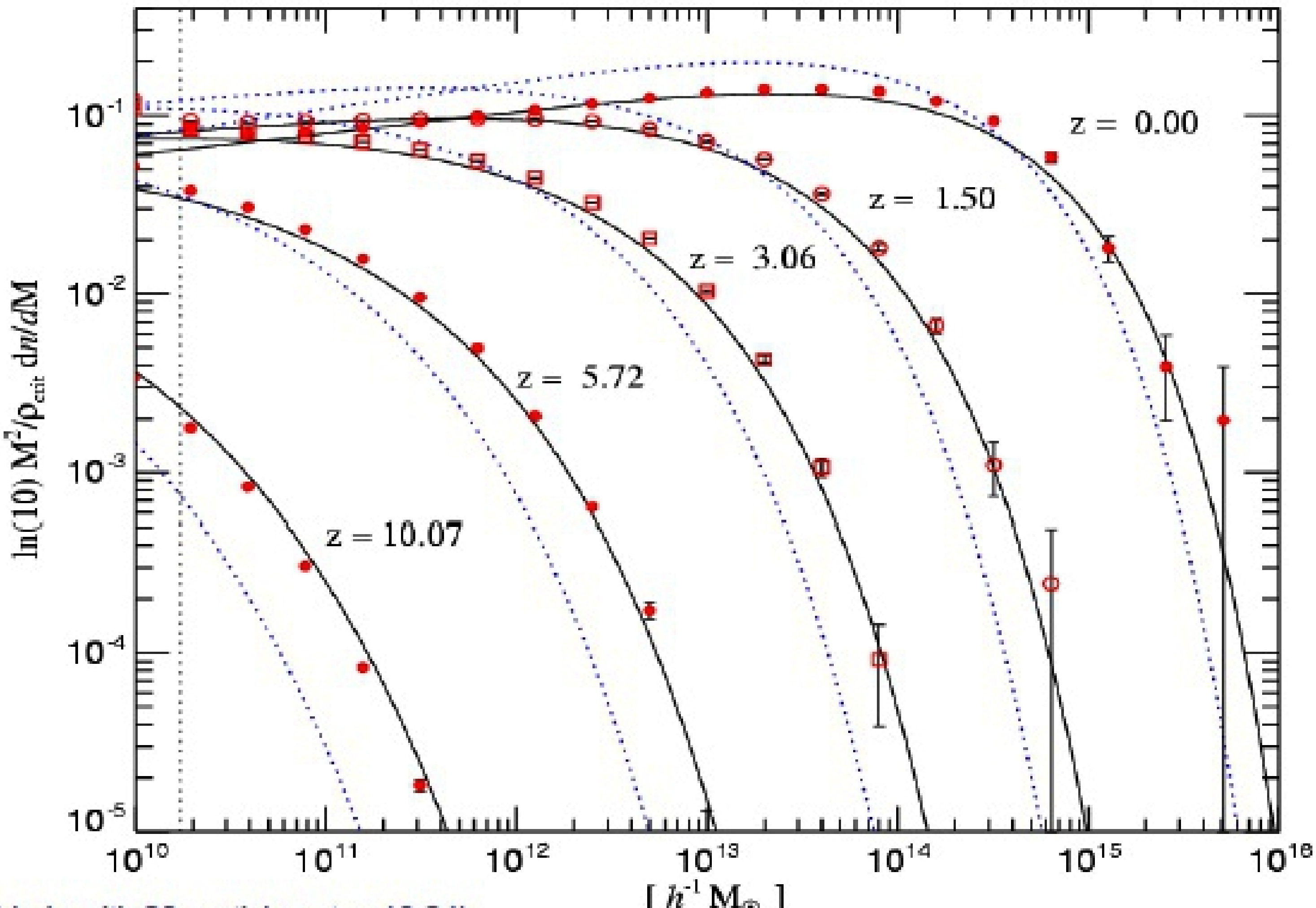

:t halo with 23 particles at z=18.24)

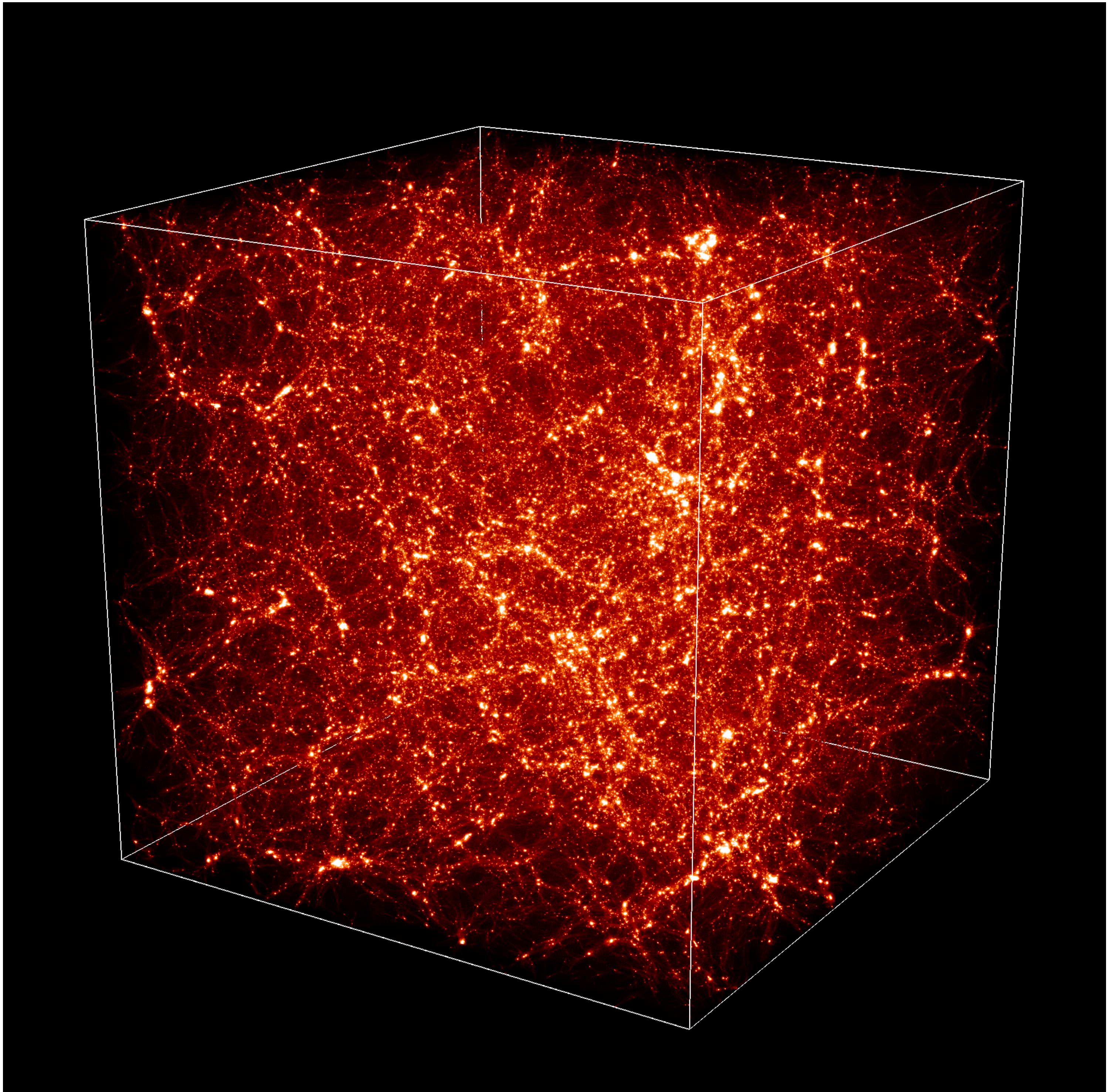

N-body simulations of gravitational clustering are the tool of choice for studying the detailed structure and dynamics of the dark matter far into the non-linear regime.

Cosmological simulations incorporate a range of physics: in this lecture, we will focus on the most basic, gravity, which is required to describe the evolution of the dark matter component. Future lecture will consider the physics applicable to the baryons.

These computations are nearly always performed using co-moving spatial coordinates and periodic boundary conditions so that a finite, expanding volume is embedded in an appropriately perturbed background space-time.

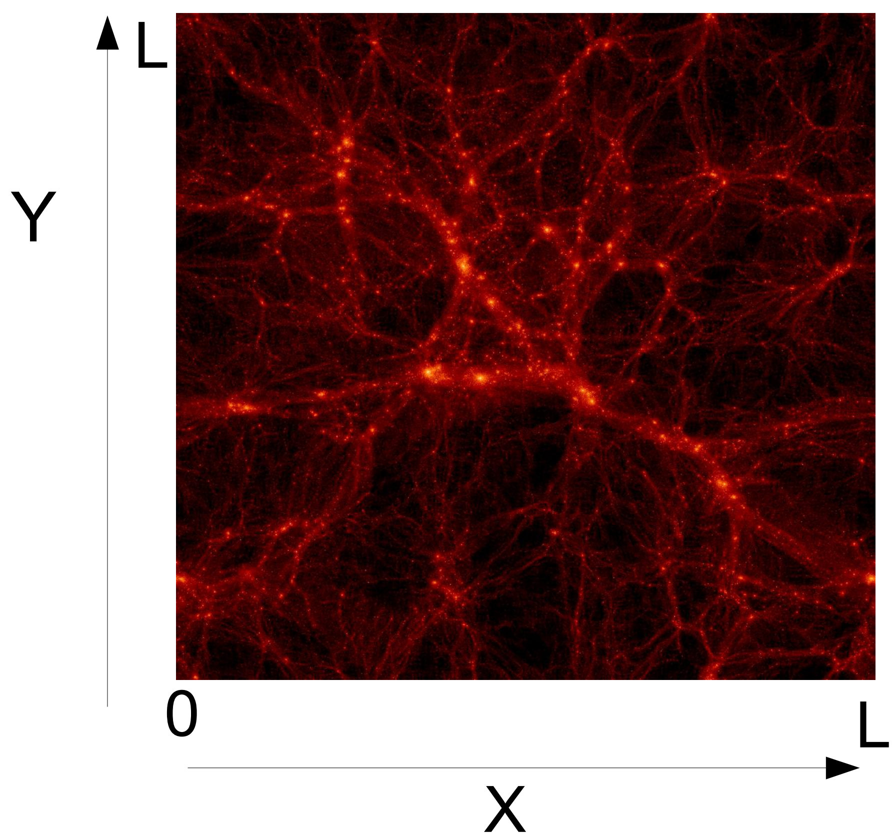

$$L + \Delta x = \Delta x$$
$$L + \Delta y = \Delta y$$

Dark matter is represented in cosmological simulations by particles sampling the phase space distribution. Particles are evolved forward in time using Newton's laws written in co-moving coordinates (Peebles 1980):

$$\frac{d\vec{x}}{dt} = \frac{1}{a}\vec{v}, \quad \frac{d\vec{v}}{dt} + H\vec{v} = \vec{g}, \quad \vec{\nabla}\cdot\vec{g} = -4\pi Ga[\rho(\vec{x},t) - \bar{\rho}(t)].$$

$\vec{v}$ is the peculiar velocity. $\vec{\nabla} = \partial/\partial\vec{x}$ is the gradient in co-moving coordinates.

The time integration of particle trajectories is generally performed using a second-order accurate leapfrog integration scheme requiring only one force evaluation per timestep. In leapfrog integration, the equations for updating position and velocitv are:

$$x_i = x_{i-1} + v_{i-1/2}\,\Delta t,$$

$$a_i = F(x_i)$$

$$v_{i+1/2} = v_{i-1/2} + a_i\,\Delta t,$$

where x_i is position at step i, $v_{i+1/2}$, is the velocity, or first derivative of x, at step i+1/2 , a_i=F(x_i) is the acceleration, or second derivative of x, at step i and Δt is the size of each time step.

There are two primary strengths to Leapfrog integration over other methods, e.g. Runge-Kutta. The first is the time-reversibility: one can integrate forward n steps, and then reverse the direction of integration and integrate backwards n steps to arrive at the same starting position. The second strength is its symplectic nature, which implies that it conserves the (slightly modified) energy of dynamical systems.

The art of N-body simulation lies chiefly in the computational algorithm used to obtain the gravitational force. Evaluating the forces by direct summation over all particle pairs is prohibitive. A variety of approximate methods are therefore employed:

1. Barnes-Hut Tree Algorithm: divides space recursively into a hierarchy of cells, each containing one or more particles. If a cell of size s and distance d (from the point where g is to be computed) satisfies $s/d < \theta$, the particles in this cell are treated as one pseudo-particle located at the center of mass of the cell. Computation is saved by replacing the set of particles by a low-order multipole expansion due to the distribution of mass in the cell.

Advantages: compute time scales as NlogN instead of N^2. Code public, spatially adaptive.

Dis-advantages: high memory requirements, does not provide periodic boundary conditions in its simplest form.

Tree algorithms approximate the force on a point with a multipole expansion

HIERARCHICAL TREE ALGORITHMS

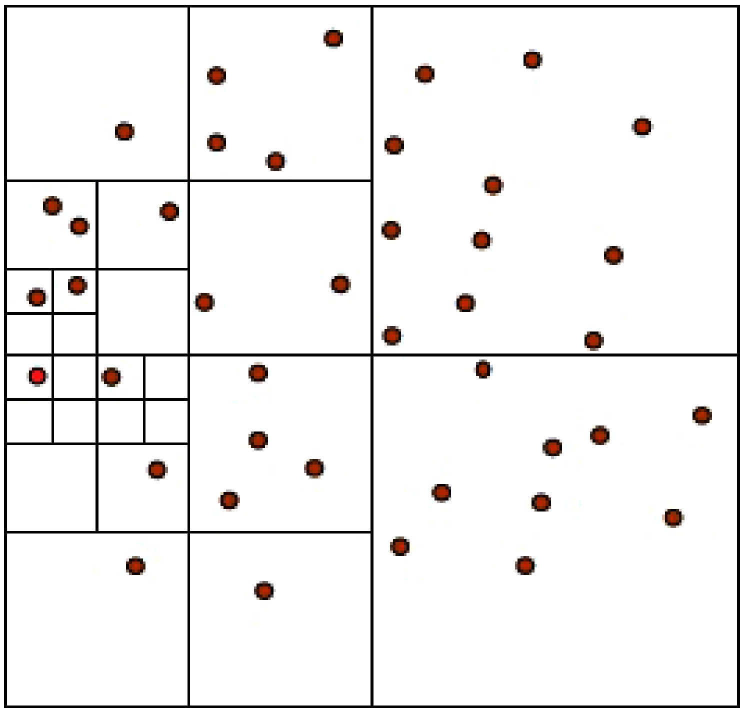

Idea: Group distant particles together, and use their multipole expansion.

→ Only ~ log(N) force terms per particle.

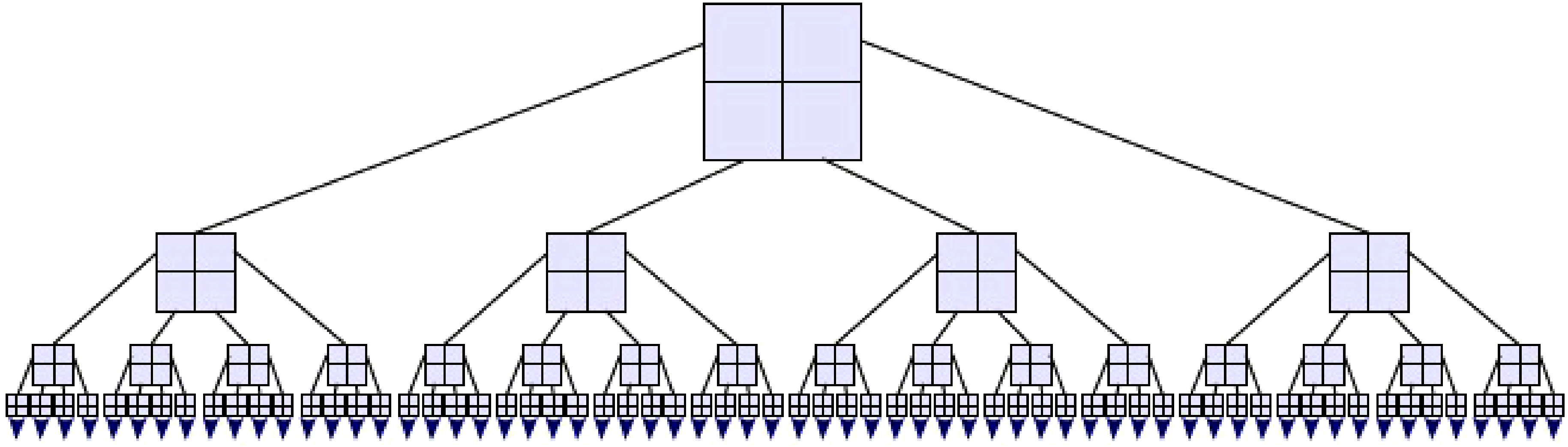

2. Particle-Mesh Algorithm. The particle-mesh (PM) method is based on representing the gravitational potential on a Cartesian grid (with a total of N_g grid points), used in solving Poisson's equation on this grid. The development of the Fast Fourier Transform (FFT) algorithm (Cooley & Tukey 1965) made possible a fast Poisson solver requiring $O(N_g \log N_g)$ operations. The algorithm consists of 3 steps:

1) Mass assignment: $\rho(\mathbf{x},t)$ is computed on the grid from discrete particle positions and masses. The most commonly used assignment scheme is Cloud-in-Cell (CIC), which uses multilinear interpolation to the eight grid points defining the cubical mesh cell containing the particle. This procedure effectively treats each particle as a uniform-density cubical cloud.

2) Calculation of the gravitational potential: The heart of the PM algorithm is the Fourier space solution of the Poisson equation for the gravitational potential.

$$\hat{\phi}(\vec{k},t) = -4\pi G a^2 \frac{\hat{\rho}(\vec{k},t)}{k^2}.$$

ρ_k and φ_k are the discrete Fourier transforms of the mass density and potential, espectively. The gravity field is then obtained by transforming the potential back to the spatial domain and approximating the gradient by finite differences.

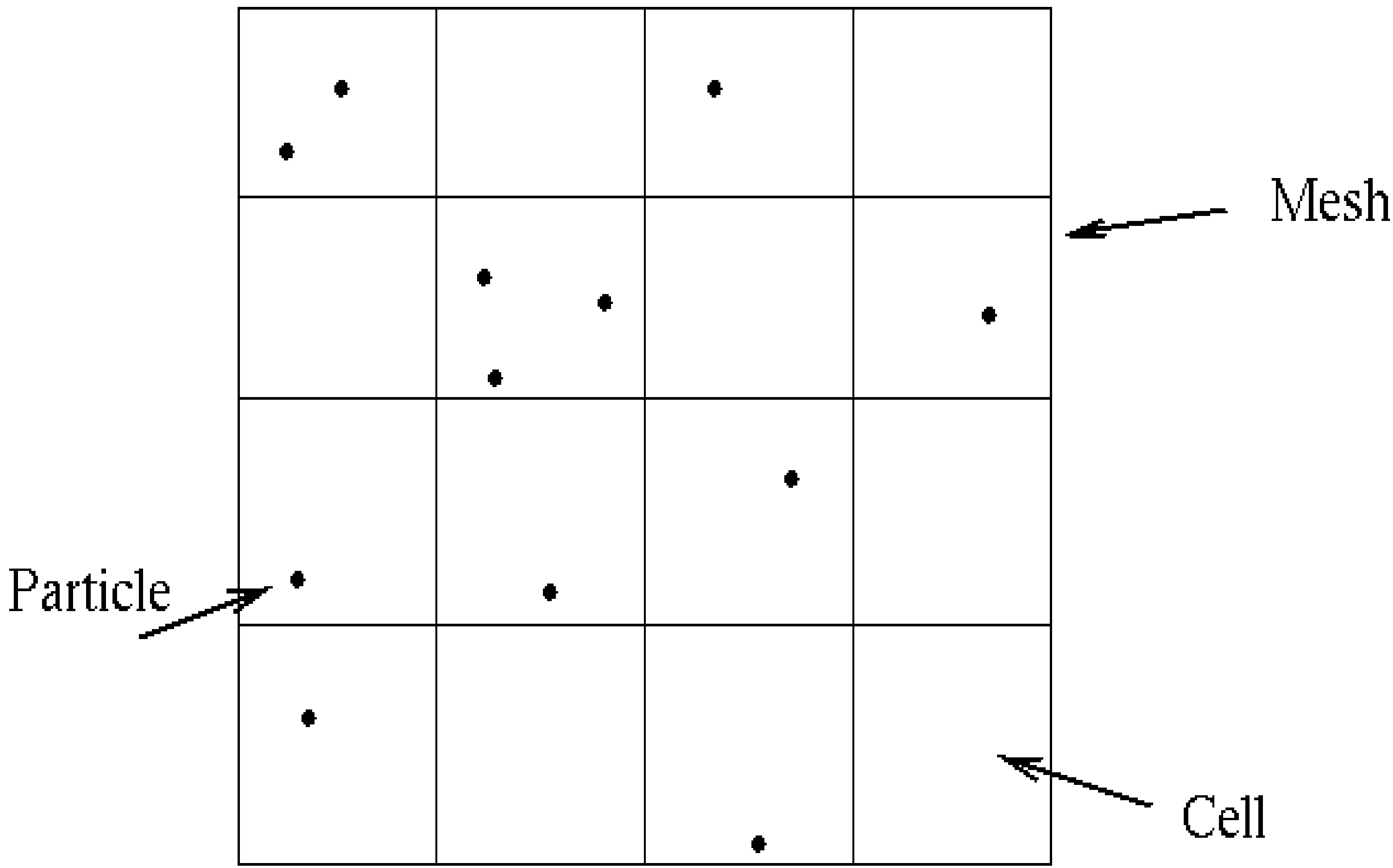
Mesh
Particle
Cell

3) Interpolate the gravity from the grid back to the particles. The same interpolation scheme should be used here as in the first step (mass assignment) to ensure that self-forces on particles vanish.

PM method advantage: Speed, requires O(N) + O(N_g log N_g) operations.
PM method disadvantage: The forces approximate the inverse square law poorly for pair separations less than several grid spacings. Each particle has an effective diameter of about two grid spacings and a non-spherical shape.

For high-resolution studies of galaxy dynamics, the tree code is generally considered much superior

Particle-Particle PM schemes (P^3M)

Idea: Supplement the PM force with a direct summation short-range force at the scale of the mesh cells. The particles in cells are linked together by a chaining list.

Offers much higher dynamic range, but becomes slow when clustering sets in.

In AP^3M, mesh-refinements are placed on clustered regions

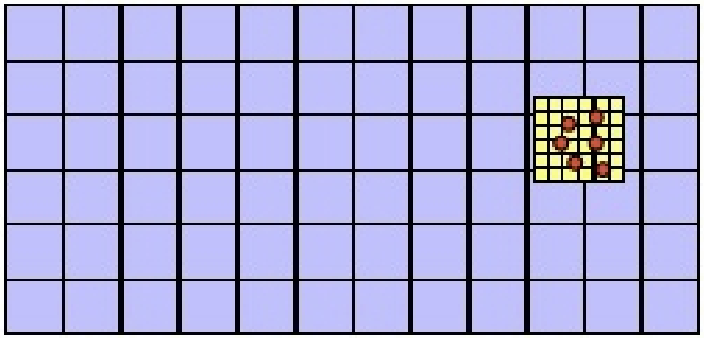

Can avoid clustering slow-down, but has higher complexity and ambiguities in mesh placement

Several groups have developed codes that automatically refine the spatial resolution where needed during the computation by using higher resolution meshes (adaptive mesh refinement).

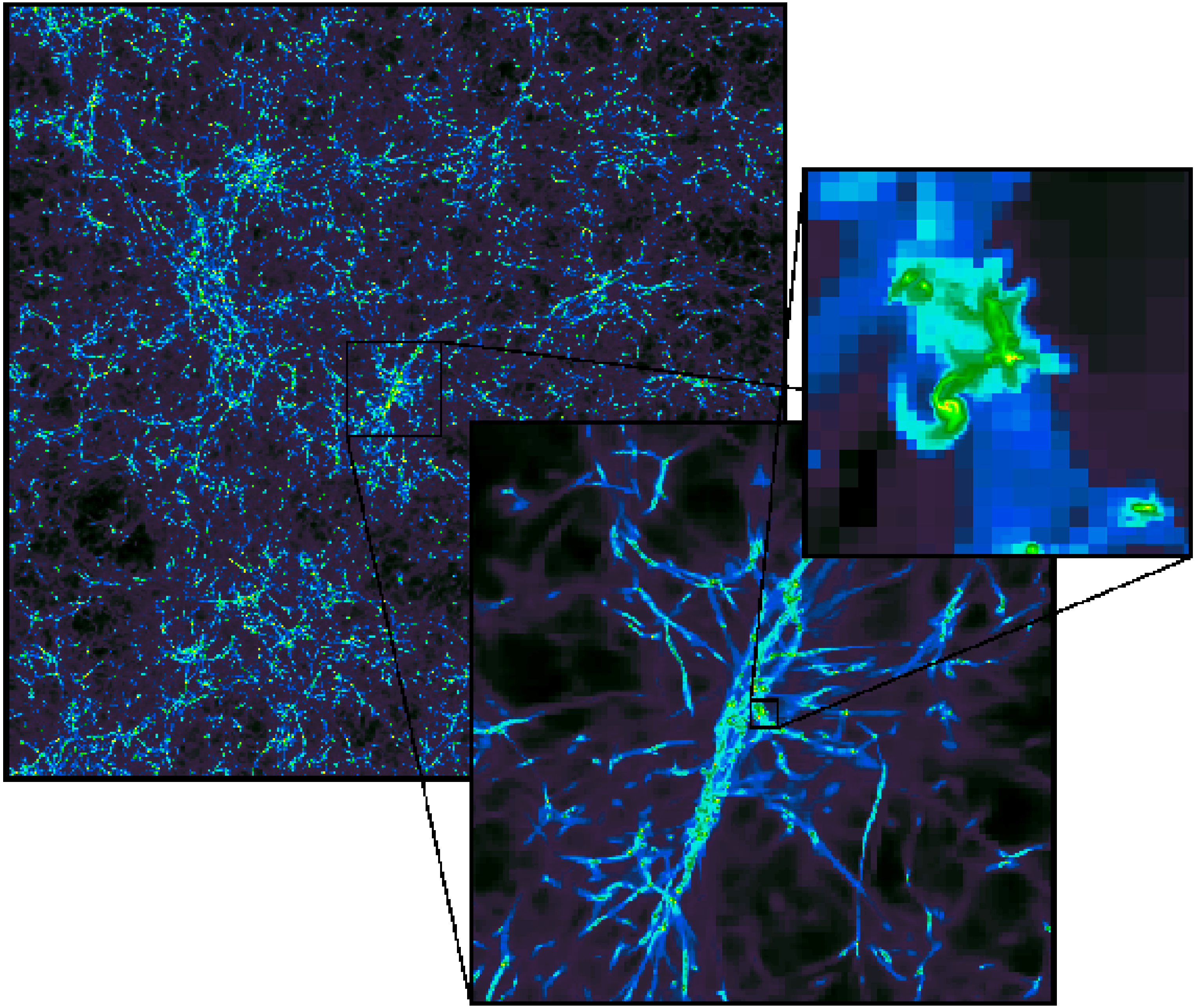

Setting up the Initial Conditions

Initial conditions for simulations of structure formation consist of specifying the background cosmological model and the perturbations imposed on this background. Gaussian fluctuations are simple, as they are specified fully by one function, the power spectrum P(k). In real space, the joint probability distribution of density fluctuations at N points is a multidimensional Gaussian. Because the covariance matrix of this Gaussian becomes diagonal in Fourier space, it is in principle easy to sample a Gaussian random field by sampling its Fourier components on a Cartesian lattice (Peacock & Heavens 1985, Bardeen et al 1986).

The standard approach for the dark matter is to displace equal-mass particles from a uniform Cartesian lattice using the Zel'dovich (1970) approximation, which describes the evolution of the density field in an approximate way. The advantage of the Zeldovich approximation is that it normally breaks down later than standard linear theory.

The Zel'dovich Approximation

Another approximate approach to the formation of structure. In this method, we work out the initial displacement of particles and assume that they continue to move in this initial direction. If the initial (Lagrangian) coordinates are called **q**, the Eulerian coordinates are given by

$$r(\mathbf{q},t) = a(t)\,[\mathbf{q} + b(t)\mathbf{s}(\mathbf{q})]$$

a(t) is the Hubble expansion. The second term is a “perturbation” term, b(t) can be thought of as the growing rate of linear fluctuations, And s(q) is a “velocity term”, which is related to the potential originated by the density fluctuations $\Phi_0(\mathbf{q})$ as

$$\mathbf{s}(\mathbf{q}) = \nabla\Phi_o(\mathbf{q})\,.$$

Mass conservation requires $\rho(\mathbf{r},t)d\mathbf{r} = \rho_0\, dq$, so that the density field As a function of Lagrangian coordinates is:

$$\rho(\mathbf{q},t) = \rho_o \left|\frac{\partial \mathbf{r}}{\partial \mathbf{q}}\right| = \frac{\bar{\rho}}{\left|\delta_{ij} - b(t)\,\frac{\partial s_i}{\partial q_j}\right|}\,.$$

$\partial r_i / \partial q_j$ describes the gravitational evolution of the density field and is called the deformation tensor.

The deformation tensor is a symmetric tensor characterized by its three eigenvalues after diagonalization, so we can write:

$$\rho(\mathbf{q}, t) = \frac{\bar{\rho}}{[1 - b(t)\,\alpha(\mathbf{q})]\,[1 - b(t)\,\beta(\mathbf{q})]\,[1 - b(t)\,\gamma(\mathbf{q})]}\,.$$

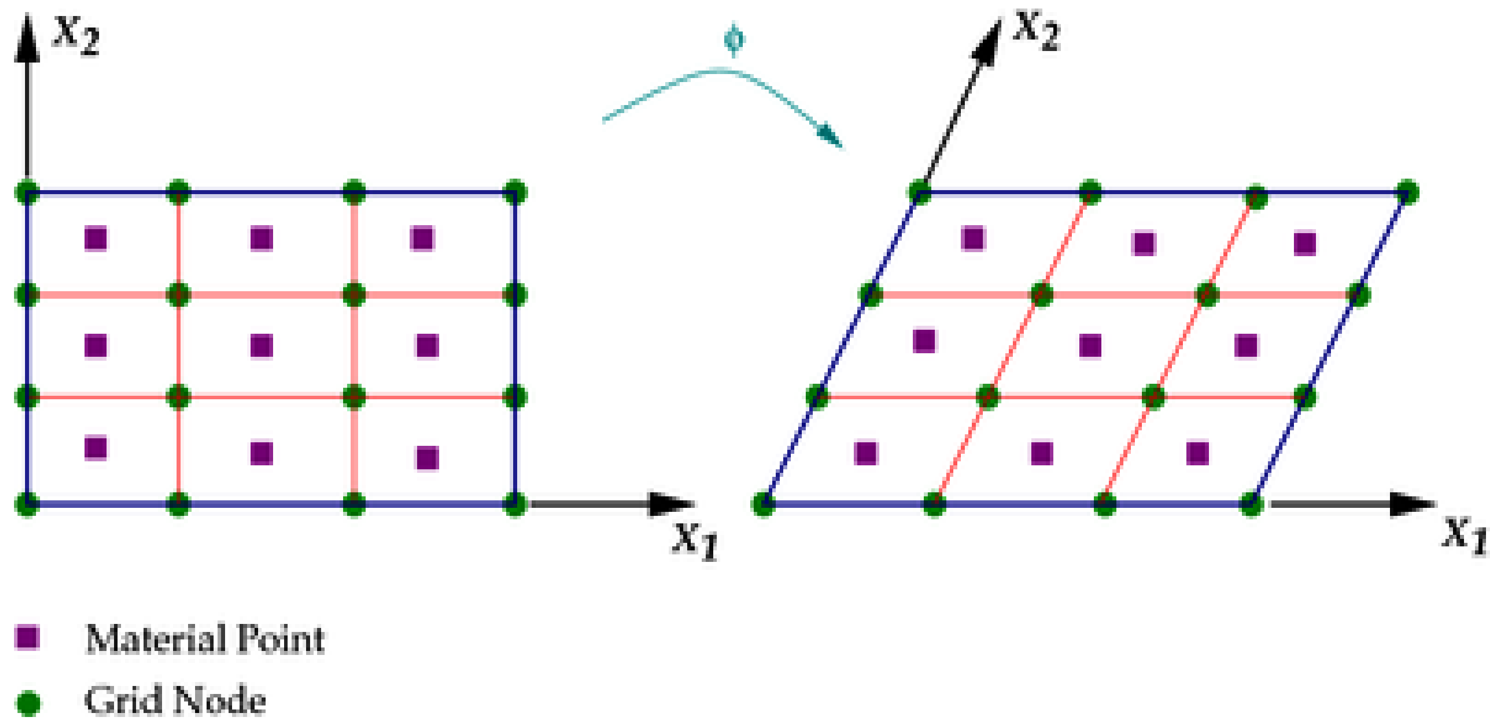

If the eigenvalues are ordered in such a way that $\alpha(\mathbf{q})>\beta(\mathbf{q})>\gamma(\mathbf{q})$, then, as b(t) grows, the first singularity occurs in correspondence of the Lagrangian coordinate $\mathbf{q}_1$ where α attains its maximum positive value α_{max}, at the time t_1 such that $b(t_1) = \alpha_{max}$-1. This corresponds to the formation of a pancake (sheet-like structure) by contraction along one of the principal axes.

The initial conditions are set up in Fourier Space.

Reason: this is convenient for Gaussian random fields.

If δ is a Gaussian random field with average 0, its probability distribution is given by:

$$P_n(\delta_1, \cdots, \delta_n) = \frac{\sqrt{\mathrm{Det}\mathbf{C}^{-1}}}{(2\pi)^{n/2}} \exp\left[-\frac{1}{2}\delta^T \mathbf{C}^{-1}\delta\right]$$

$$\mathbf{C}_{ij} = \langle \delta_i \delta_j \rangle.$$

Multi-variate Gaussian

1. A Gaussian random field in Fourier space is still Gaussian

$$P(|\delta_{\mathbf{k}}|^2 > X) = \int_{\sqrt{X}}^{\infty} \frac{1}{\sigma_k^2} \exp\left[-\frac{|\delta_{\mathbf{k}}|^2}{2\sigma_k^2}\right] |\delta_{\mathbf{k}}| d|\delta_{\mathbf{k}}| = \exp\left[-\frac{X}{\langle |\delta_{\mathbf{k}}|^2 \rangle}\right]$$

2. Phases of the Fourier modes are random

.

Using the Zeldovich approximation, density fluctuations are converted to displacements of the unperturbed particle load

SETTING INITIAL DISPLACEMENTS AND VELOCITIES

Particle displacements: $\mathbf{d}_i(t) = \mathbf{x}_i(t) - \mathbf{q}_i$

Density change due to displacements: $\rho(\mathbf{x}) = \frac{\rho_0}{\left|\frac{\partial \mathbf{x}}{\partial \mathbf{q}}\right|} = \frac{\rho_0}{\left|\delta_{ij} + \frac{\partial \mathbf{d}}{\partial \mathbf{q}}\right|}$

For small displacements: $\left|\delta_{ij} + \frac{\partial \mathbf{d}}{\partial \mathbf{q}}\right| \simeq 1 + \nabla_{\mathbf{q}} \cdot \mathbf{d}$

Resulting density contrast: $\delta(\mathbf{x}) = \frac{\rho(\mathbf{x}) - \rho_0}{\rho} = -\nabla_{\mathbf{q}} \cdot \mathbf{d}$

During linear growth:

$$\delta(t) = D(t)\delta_0$$

$$\mathbf{d}(t) = D(t)\mathbf{d}_0$$

$$\Rightarrow \quad \dot{\mathbf{x}} = \dot{\mathbf{d}} = \dot{a}\frac{\mathrm{d}D}{\mathrm{d}a}\mathbf{d}_0 = \frac{\dot{a}}{a}\frac{a}{D}\frac{\mathrm{d}D}{\mathrm{d}a}\mathbf{d}$$

Particle velocities:

$$\dot{\mathbf{x}} = H(a) f(\Omega)\mathbf{d} \qquad f(\Omega) = \frac{\mathrm{d}\ln D}{\mathrm{d}\ln a} \simeq \Omega^{0.6}$$

Note: Particles move on straight lines in the Zeldovich approximation.

Displacement field: $\nabla^2 \phi = \delta \qquad \mathbf{d} = -\nabla\phi$

Fourier realization:

$$\phi_{\mathbf{k}} = -\frac{1}{k^2}\delta_{\mathbf{k}} \qquad \mathbf{d}_{\mathbf{k}} = -i\mathbf{k}\phi_{\mathbf{k}} = \frac{i\mathbf{k}}{k^2}\delta_{\mathbf{k}} \qquad \mathbf{d}_{\mathbf{k}} = -\nabla\phi = \sum_{\mathbf{k}} \frac{i\mathbf{k}\delta_{\mathbf{k}}}{k^2}\exp(i\mathbf{k}\mathbf{x})$$

During linear growth:

$$\delta(t) = D(t)\delta_0$$
$$\mathbf{d}(t) = D(t)\mathbf{d}_0$$

$$\Rightarrow \quad \dot{\mathbf{x}} = \dot{\mathbf{d}} = \dot{a}\frac{\mathrm{d}D}{\mathrm{d}a}\mathbf{d}_0 = \frac{\dot{a}}{a}\frac{a}{D}\frac{\mathrm{d}D}{\mathrm{d}a}\mathbf{d}$$

The linear theory power spectrum can be computed accurately

THE APPROXIMATE SHAPE OF THE LINEAR POWER SPECTRUM

$$P(k) = A\frac{k^n}{\{1 + [ak/\Gamma + (bk/\Gamma)^{3/2} + (ck/\Gamma)^2]^\nu\}^{1/\nu}}$$

Standard LCDM:
$$n = 1.0$$
$$\Gamma = 0.21$$
$$a = 6.4\ h^{-1}\mathrm{Mpc}$$
$$b = 3.0\ h^{-1}\mathrm{Mpc}$$
$$c = 1.7\ h^{-1}\mathrm{Mpc}$$
$$\nu = 1.13$$

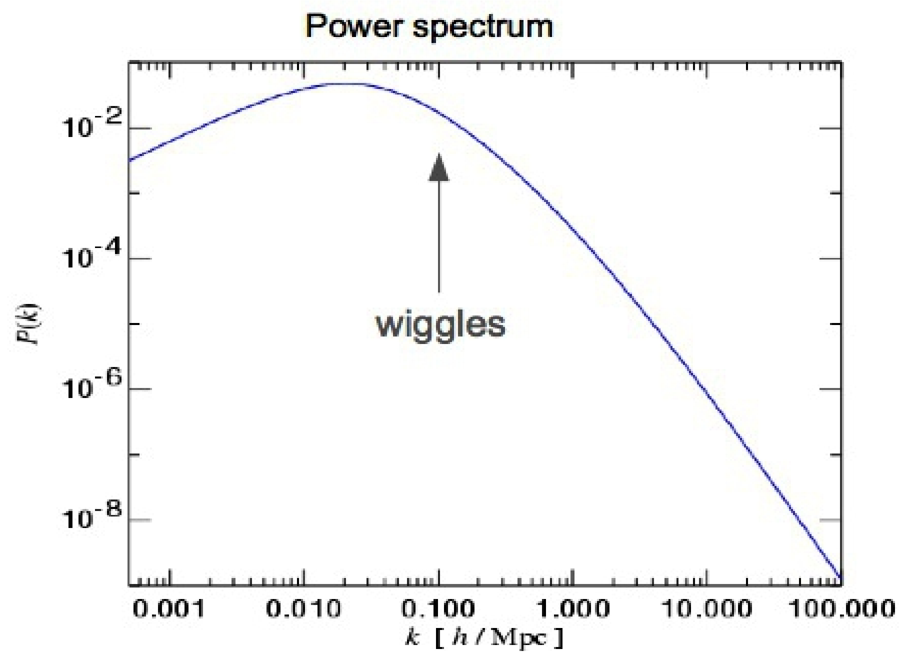

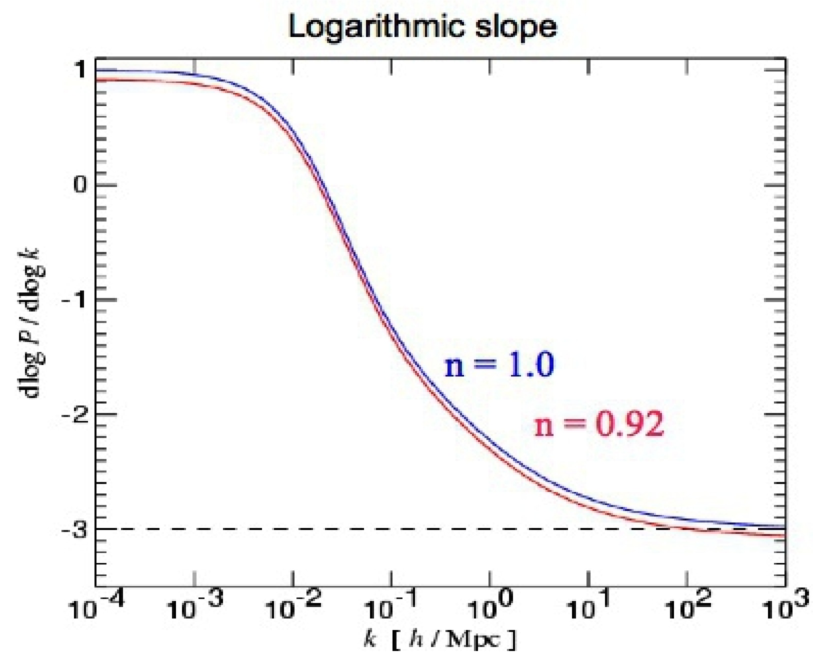

To determine the power spectrum amplitude, we normalize the spectrum to observations of clustering (usually galaxy clusters)

FILTERED DENSITY FIELD AND THE NORMALIZATION OF THE POWER SPECTRUM

The filtered density field:

$$\sigma^2(M,z) = D^2(z)\int_0^\infty \frac{\mathrm{d}k}{2\pi^2}k^2P(k)\left[\frac{3j_1(kR)}{kR}\right]^2$$

Observational input:

$$\sigma_8 = 0.74 - 0.9 \qquad R = 8\,h^{-1}\mathrm{Mpc}$$

Extrapolate back to the starting redshift with the growth factor D(z)
This depends on cosmology.

→ fluctuation spectrum of initial conditions fully specified.

When particles are distributed initially on a lattice, the small-scale periodicity of the lattice persists visibly until virialization occurs, i.e. until particles fall into and orbit in gravitationally bound objects. To avoid this artificial pattern, before applying displacements, particles can be arranged in a random "glass" state with very small gravitational forces. A gravitational glass is made by advancing particles from random positions using the opposite sign of gravity until they "freeze" in co-moving coordinates (Baugh et al 1995, White 1996).

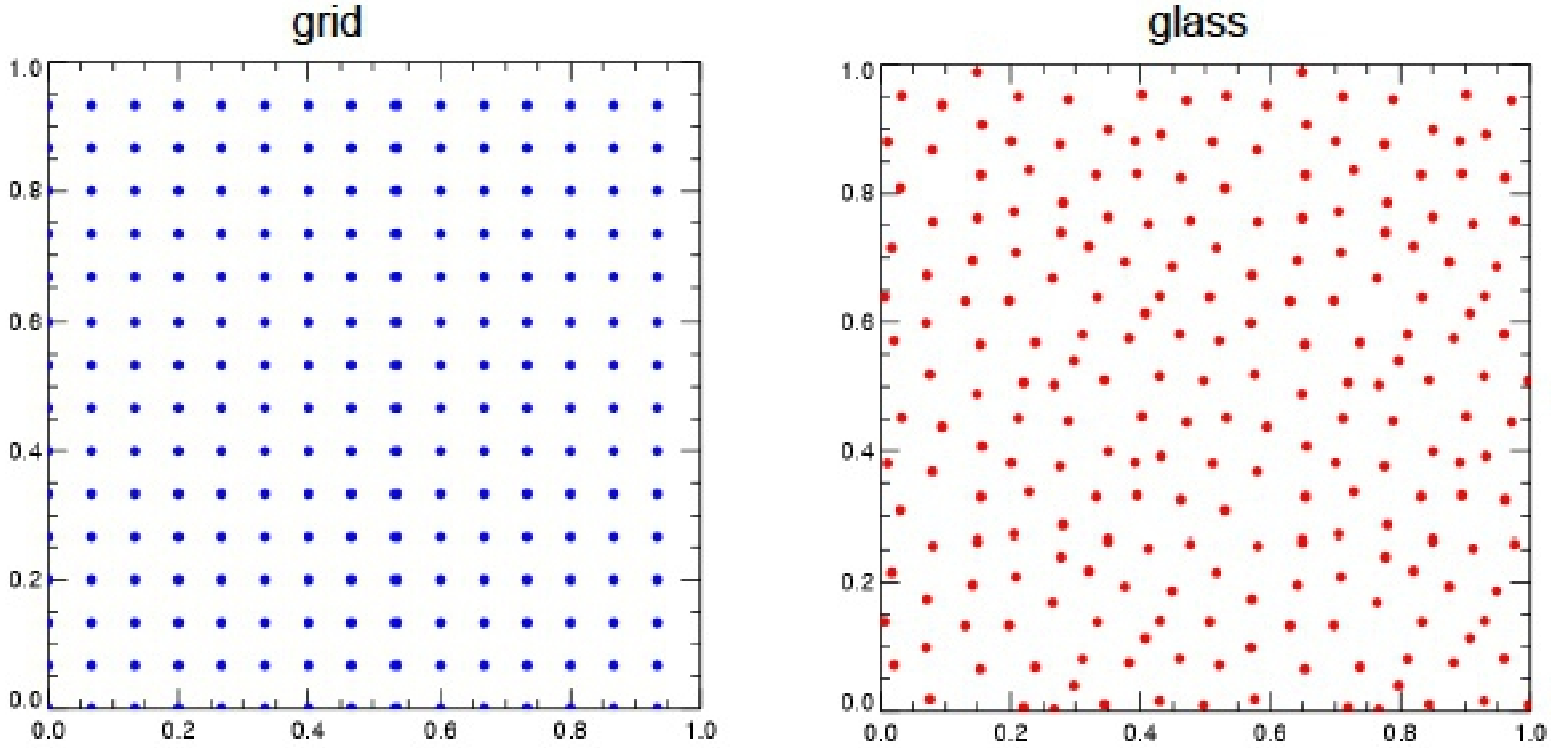

One usually assigns random amplitudes and phases for individual modes in Fourier space

GENERATING THE FLUCTUATIONS IN K-SPACE

Simulation box

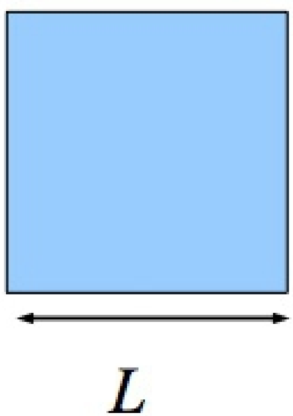

sampled with
N^2 points

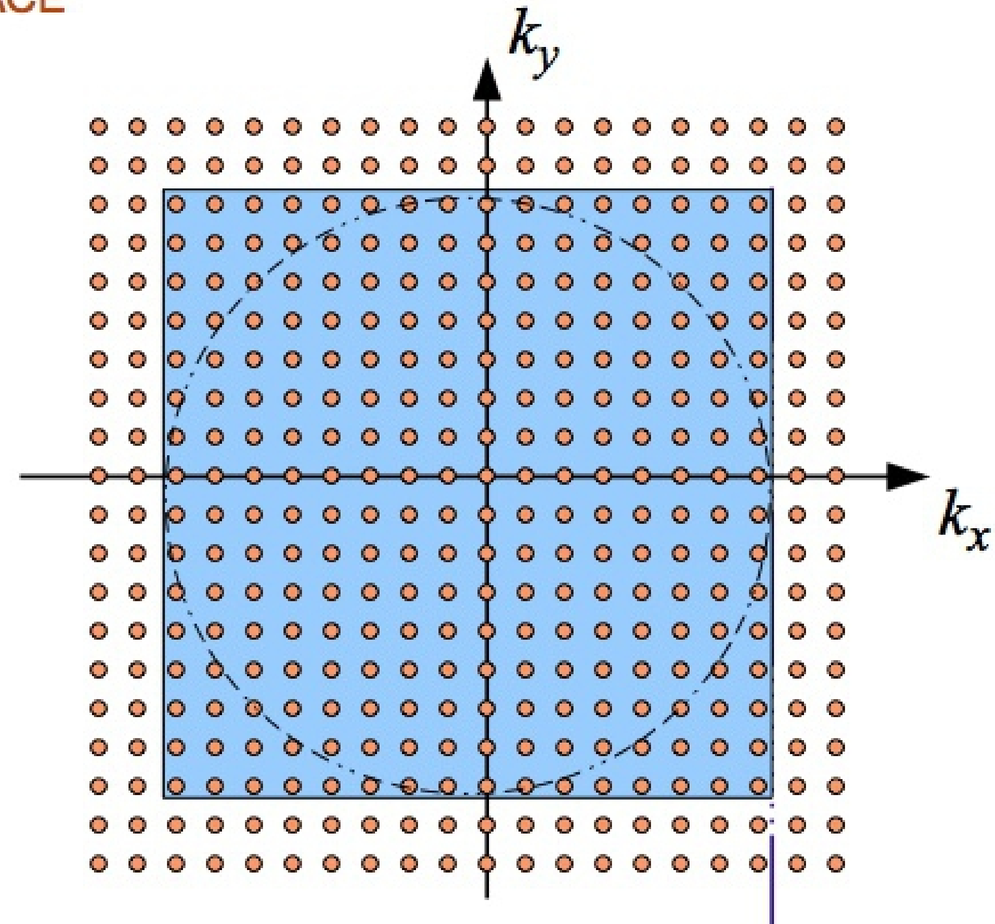

$$k_{\rm Nyquist} = \frac{2\pi}{L}\,\frac{N}{2}$$

$$\delta_{\mathbf{k}} = B_{\mathbf{k}} \exp^{\mathrm{i}\,\phi_{\mathbf{k}}}$$

For each mode, draw a random phase, and an amplitude from a Rayleigh distribution.

$$\left\langle \delta_{\mathbf{k}}^2 \right\rangle = P(k)$$

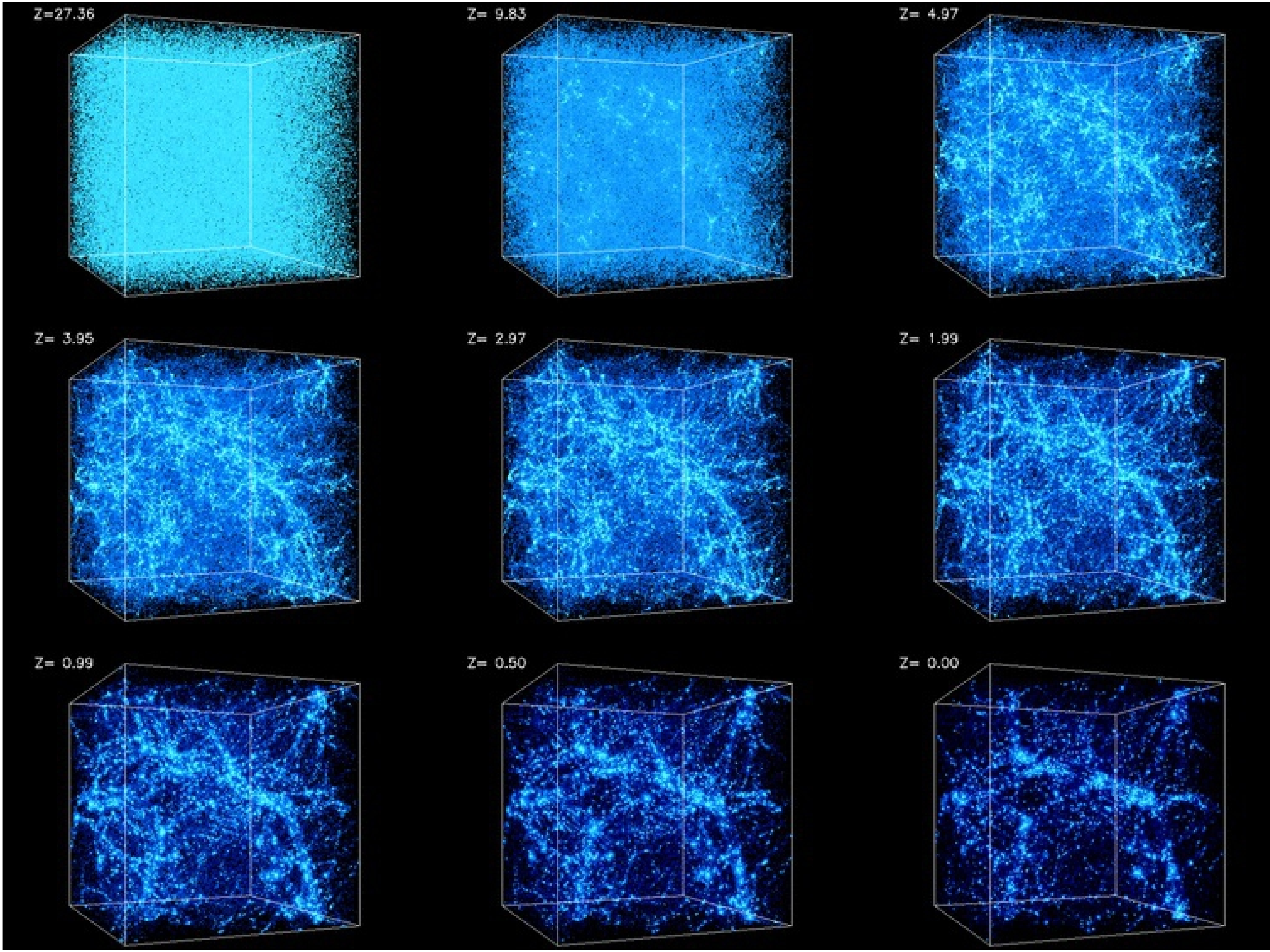
Z=27.36
Z= 9.83
Z= 4.97
Z= 3.95
Z= 2.97
Z= 1.99
Z= 0.99
Z= 0.50
Z= 0.00

Other structures like filaments and knots come from simultaneous contractions along two and three axes, respectively. The approximation holds quite well for the first collapse, but breaks down at late times for power spectra with significant power on small scales (i.e. in the regime of hierarchical clustering).

N-body

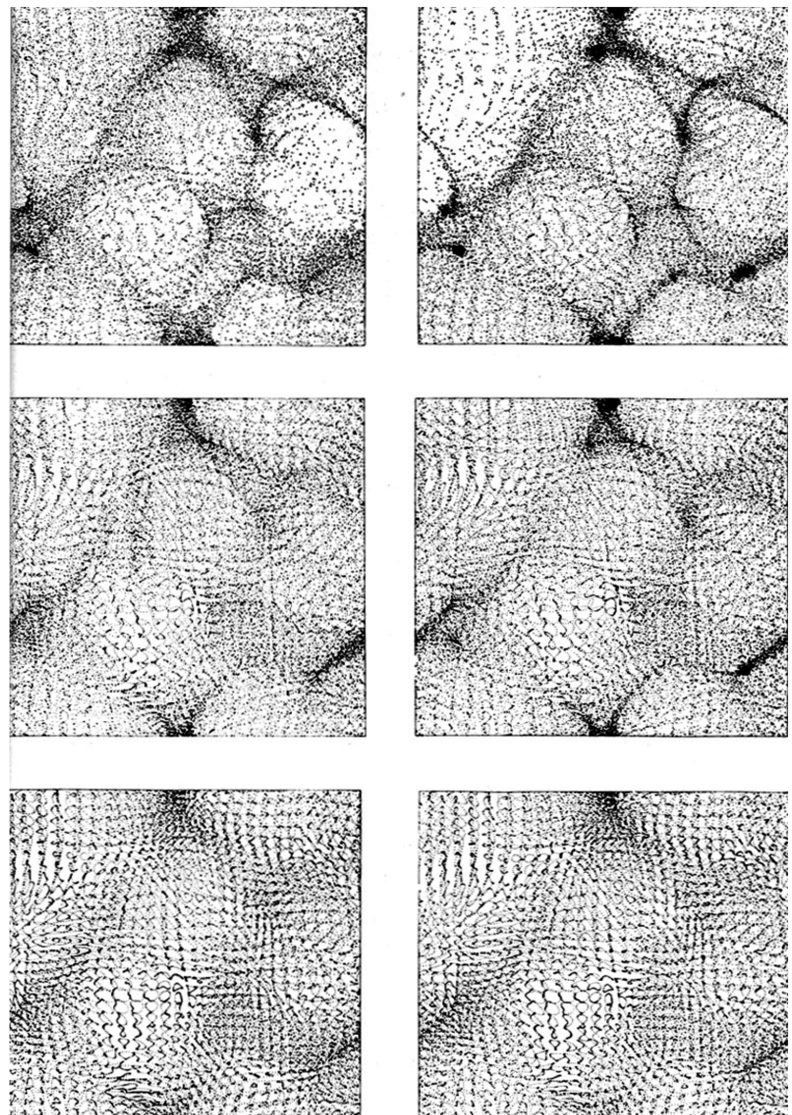

Zel'dovich

LIMITATIONS OF N-BODY SIMULATIONS

In purely gravitational N-body simulations of structure formation, the numerical issues include dynamic range, force accuracy, and time integration accuracy. Of these, dynamic range is the most difficult to deal with:

Three distinct kinds of dynamic range are needed for a faithful simulation: mass resolution (number of particles), initial power spectrum sampling (range of wavenumbers present in the initial conditions), and spatial resolution (force-softening length compared with box size). The era of parallelization of codes and ever-increasing supercomputer power have allowed enormous advances over what was possible in the 1980's and 1990's. This will be described in the next lecture.

Cosmological N-body simulations have grown rapidly in size over the last three decades

"N" AS A FUNCTION OF TIME

- Computers double their speed every 18 months (Moore's law)
- N-body simulations have doubled their size every 16-17 months
- Recently, growth has accelerated further.
  The Millennium Run should have become possible in 2010 – we it was done in 2004.
  It took ~350000 CPU hours, about a month on 512 cores.